

$(\alpha/\beta+\alpha)$ -Peptide Antagonists of BH3 Domain/Bcl-x_L Recognition: Toward General Strategies for Foldamer-Based Inhibition of Protein–Protein Interactions

Jack D. Sadowsky,[†] W. Douglas Fairlie,[‡] Erik B. Hadley,[†] Hee-Seung Lee,^{†,‡}
Naoki Umezawa,^{†,§} Zaneta Nikolovska-Coleska,[§] Shaomeng Wang,[§]
David C. S. Huang,[‡] York Tomita,^{*,||} and Samuel H. Gellman^{*,†}

Contribution from the Department of Chemistry, University of Wisconsin, Madison, Wisconsin 53706, The Walter and Eliza Hall Institute of Medical Research, Parkville, Victoria 3050, Australia, Departments of Internal Medicine and Medicinal Chemistry, University of Michigan, Ann Arbor, Michigan 48109, and Lombardi Comprehensive Cancer Center, Georgetown University Medical Center, Washington, DC 20057

Received August 31, 2006; E-mail: gellman@chem.wisc.edu; yat@georgetown.edu

Abstract: The development of molecules that bind to specific protein surface sites and inhibit protein–protein interactions is a fundamental challenge in molecular recognition. New strategies for approaching this challenge could have important long-term ramifications in biology and medicine. We are exploring the concept that unnatural oligomers with well-defined conformations (“foldamers”) can mimic protein secondary structural elements and thereby block specific protein–protein interactions. Here, we describe the identification and analysis of helical peptide-based foldamers that bind to a specific cleft on the anti-apoptotic protein Bcl-x_L by mimicking an α -helical BH3 domain. Initial studies, employing a fluorescence polarization (FP) competition assay, revealed that among several α/β - and β -peptide foldamer backbones only α/β -peptides intended to adopt 14/15-helical secondary structure display significant binding to Bcl-x_L. The most tightly binding Bcl-x_L ligands are chimeric oligomers in which an N-terminal α/β -peptide segment is fused to a C-terminal α -peptide segment ($(\alpha/\beta+\alpha)$ -peptides). Sequence–affinity relationships were probed via standard and nonstandard techniques (alanine scanning and hydrophile scanning, respectively), and the results allowed us to construct a computational model of the ligand/Bcl-x_L complex. Analytical ultracentrifugation with a high-affinity $(\alpha/\beta+\alpha)$ -peptide established 1:1 ligand:Bcl-x_L stoichiometry under FP assay conditions. Binding selectivity studies with the most potent $(\alpha/\beta+\alpha)$ -peptide, conducted via surface plasmon resonance measurements, revealed that this ligand binds tightly to Bcl-w as well as to Bcl-x_L, while binding to Bcl-2 is somewhat weaker. No binding could be detected with Mcl-1. We show that our most potent $(\alpha/\beta+\alpha)$ -peptide can induce cytochrome C release from mitochondria, an early step in apoptosis, in cell lysates, and that this activity is dependent upon inhibition of protein–protein interactions involving Bcl-x_L.

Introduction

Selective interactions between proteins are vital in biological processes. Molecules that bind to specific protein surface sites and thereby disrupt protein–protein interactions are potentially useful as tools for basic biological research and as medicinal agents. Extensive efforts to develop antagonists for a variety of protein–protein interactions have revealed that this type of goal is often difficult to accomplish via traditional medicinal chemistry strategies, that is, strategies that rely on molecules of relatively low molecular weight.¹ In contrast, decades of research have shown that small molecule-based approaches are

quite effective for blocking other types of protein-dependent processes, such as catalysis; many potent enzyme inhibitors are in clinical use.² Most medicinally targeted enzyme active sites are protein surfaces that have evolved to bind to substrates of low molecular weight, a characteristic that makes these sites intrinsically susceptible to small-molecule inhibitors.

The development of protein–protein interaction antagonists represents a fundamental challenge in molecular recognition that differs from the challenge inherent in enzyme inhibitor design.¹ Of particular importance are protein–protein interfaces at which large surfaces (>500 Å²) are buried; in such cases, the recognition surfaces have evolved to bind partners of high molecular weight, which makes development of small-molecule

[†] University of Wisconsin.

[‡] The Walter and Eliza Hall Institute of Medical Research.

[§] University of Michigan.

^{||} Georgetown University Medical Center.

^{*} Current address: Korea Advanced Institute of Science and Technology, Korea.

[#] Current address: Nagoya City University, Japan.

- (1) (a) Arkin, M. R.; Wells, J. A. *Nat. Rev. Drug Discovery* **2004**, *3*, 301–317. (b) Cochran, A. G. *Chem. Biol.* **2000**, *7*, R85–R94. (c) Gadek, T. R.; Nicholas, J. B. *Biochem. Pharmacol.* **2003**, *65*, 1–8. (d) Berg, T. *Angew. Chem., Int. Ed.* **2003**, *42*, 2462–2481. (e) Peczu, M. W.; Hamilton, A. D. *Chem. Rev.* **2000**, *100*, 2479–2494.
(2) (a) Babine, R. E.; Bender, S. L. *Chem. Rev.* **1997**, *97*, 1359–1472. (b) Bursavich, M. G.; Rich, D. H. *J. Med. Chem.* **2002**, *45*, 541–558.

inhibitors intrinsically difficult. Although impressive small-molecule antagonists have been reported for a few such interactions,^{1,3} clinical success to date has been achieved with only protein or large peptide antagonists.^{4,5} Such macromolecular agents can be difficult to produce in pure form and can suffer from low stability during storage and/or upon administration. Thus, it is important to explore new strategies for protein–protein interaction inhibitor development. Exploration must begin at a basic level, involving experiments with purified proteins, to generate molecular-level understanding that can support subsequent cell- and organism-based efforts. The history of enzyme inhibitor development shows the importance of fundamental protein-based studies for elucidating mechanisms of action and identifying key design parameters.²

Our broad goal is to evaluate foldamers (oligomers with well-defined folding propensities)⁶ as a source of molecules that can bind tightly and selectively to surface sites on proteins. If foldamers can be targeted to sites that normally recognize other proteins, then these foldamers may inhibit protein–protein binding. A variety of foldamers have been shown to adopt discrete and predictable secondary structures, most prominently helices.^{6–8} α -Helical motifs are commonly found at interfaces between proteins,⁹ and it is reasonable to propose that helical oligomers with unnatural backbones and appropriate side chains might mimic the recognition surfaces displayed by natural α -helices. The research presented below focuses in particular on Bcl-2 family protein interactions, in which an α -helical segment (“BH3 domain”) from one partner binds into a long complementary cleft on the other.

Interactions between proteins of the Bcl-2 family influence whether a cell will live or die in response to stress.¹⁰ Pro-apoptotic (pro-death) Bcl-2 family members such as Bak, Bax, Bad, Bid, Bim, Noxa, and Hrk induce cell death by directly (e.g., Bak, Bax) or indirectly (e.g., Bad, Bid, Bim) causing permeabilization of mitochondrial membranes, release of apoptogenic factors (e.g., cytochrome C) into the cytosol, and activation of caspases. Anti-apoptotic Bcl-2 family proteins such as Bcl-x_L, Bcl-2, Bcl-w, Mcl-1, and A1 inhibit cell death by binding to the highly conserved Bcl-homology 3 (BH3) domain of pro-apoptotic family members. In several types of cancer,

anti-apoptotic Bcl-2 family proteins are overexpressed and can saturate pro-apoptotic family members, resulting in protection of malignant cells from the cytotoxic effects of chemotherapy and radiation.^{10d} For this reason, many groups have sought molecules that antagonize interaction of the BH3 domain of a pro-apoptotic Bcl-2 family member with the BH3-recognition site on an anti-apoptotic family member.¹¹ Short peptides (~16–33 α -amino acid residues) derived from pro-apoptotic BH3 domains bind tightly, in an α -helical conformation, to anti-apoptotic Bcl-2 family proteins, burying >800 Å² of surface area upon complexation.^{12–14} Small molecules that target the BH3-recognition site on anti-apoptotic Bcl-2 family proteins have been discovered through library screening, although most of the reported small molecules bind significantly less tightly than do BH3-derived α -peptides.¹¹ Recently, however, a very potent class of small-molecule ligands for Bcl-x_L, Bcl-2, and Bcl-w ($K_d \approx 1$ nM) was reported.^{3c} Tris-pyridylamides,^{15a} terephthalamides,^{15b} and terphenyls,^{15c} rationally designed to mimic side chain display from the α -helical structure of BH3 domains, show affinity for anti-apoptotic proteins Bcl-2 and Bcl-x_L that approach the affinity of some naturally derived BH3 domain α -peptides.

Wells and Arkin have pointed out that application of multiple physical tools is required to establish and elucidate the mechanism by which synthetic ligands bind to protein recognition sites and disrupt protein–protein interactions.^{1a} In this regard, the BH3-recognition cleft of Bcl-x_L represents an excellent target for fundamental studies directed toward α -helix mimicry by foldamers. Soluble forms of Bcl-x_L are readily expressed, and high-resolution structural data are available for the protein alone and bound to BH3 domain peptides.^{12,14} Several peptides corresponding to natural BH3 domains bind to Bcl-x_L;¹⁶ sequence comparisons among these ligands, along with mutational studies of these ligands, can be used to guide the design of foldameric antagonists. BH3 domain binding preferences vary considerably among Bcl-x_L and related anti-apoptotic proteins

- (3) (a) Thanos, C.; Randal, M.; Wells, J. A. *J. Am. Chem. Soc.* **2003**, *125*, 15280–15281. (b) Vassilev, L. T.; Vu, B. T.; Graves, B.; Carvajal, D.; Podlaski, F.; Filipovic, Z.; Kong, N.; Kammlott, U.; Lukacs, C.; Klein, C.; Fotouhi, N.; Liu, E. A. *Science* **2004**, *303*, 844–848. (c) Oltersdorf, T.; et al. *Nature* **2005**, *435*, 677–681.
- (4) Ferrara, N.; Hillan, K. J.; Gerber, H.-P.; Novotny, W. *Nat. Rev. Drug Discovery* **2004**, *3*, 391–400.
- (5) Matthews, T.; Salgo, M.; Greenberg, M.; Chung, J.; DeMasi, R.; Bolognesi, D. *Nat. Rev. Drug Discovery* **2004**, *3*, 215–225.
- (6) Gellman, S. H. *Acc. Chem. Res.* **1998**, *31*, 173–180.
- (7) A review of several foldamer architectures: Hill, D. J.; Mio, M. J.; Prince, R. B.; Hughes, T. S.; Moore, J. S. *Chem. Rev.* **2001**, *101*, 3893–4011.
- (8) α/β -Peptide secondary structures: (a) Hayen, A.; Schmitt, M. A.; Ngassa, F. N.; Thomasson, K. A.; Gellman, S. H. *Angew. Chem., Int. Ed.* **2004**, *43*, 505–510. (b) Schmitt, M. A.; Choi, S. H.; Guzei, I. A.; Gellman, S. H. *J. Am. Chem. Soc.* **2005**, *127*, 13130–13131. (c) De Pol, S.; Zorn, C.; Klein, C. D.; Zerbe, O.; Reiser, O. *Angew. Chem., Int. Ed.* **2004**, *43*, 511–514. (d) Sharma, G. V. M.; Nagendar, P.; Jayaprakash, P.; Krishna, P. R.; Ramakrishna, K. V. S.; Kunwar, A. C. *Angew. Chem., Int. Ed.* **2005**, *44*, 5878–5882. β -Peptide secondary structures: (e) Baldauf, C.; Gunther, R.; Hofmann, H.-J. *Biopolymers* **2006**, *84*, 408–413. (f) Cheng, R. P.; Gellman, S. H.; DeGrado, W. F. *Chem. Rev.* **2001**, *101*, 3219–3232.
- (9) Oldfield, C. J.; Cheng, Y.; Cortese, M. S.; Romero, P.; Uversky, V. N.; Dunker, A. K. *Biochemistry* **2005**, *44*, 12454–12470.
- (10) (a) Adams, J. M.; Cory, S. *Science* **1998**, *281*, 1322–1326. (b) Coultas, L.; Strasser, A. *Semin. Cancer Biol.* **2003**, *13*, 115–123. (c) Letai, A.; Bassik, M. C.; Walensky, L. D.; Sorcinelli, M. D.; Weiler, S.; Korsmeyer, S. J. *Cancer Cell* **2002**, *2*, 183–192. (d) Dharap, S. S.; Chandna, P.; Wang, Y.; Khandare, J. J.; Qiu, B.; Stein, S.; Minko, T. *J. Pharmacol. Exp. Ther.* **2006**, *316*, 992–998.
- (11) Reviews of approaches to Bcl-x_L inhibition: (a) Baell, J. B.; Huang, D. C. S. *Biochem. Pharmacol.* **2002**, *64*, 851–863. (b) O’Neill, J.; Manion, M.; Schwartz, P.; Hockenbery, D. M. *Biochim. Biophys. Acta* **2004**, *1705*, 43–51.
- (12) A review of high-resolution structural characterization of BH3/Bcl-x_L interactions: Petros, A. M.; Olejniczak, E. T.; Fesik, S. W. *Biochim. Biophys. Acta* **2004**, *1644*, 83–94.
- (13) (a) Wang, D.; Liao, W.; Arora, P. S. *Angew. Chem., Int. Ed.* **2005**, *44*, 6525–6529. (b) Gemperli, A. C.; Rutledge, S. E.; Maranda, A.; Schepartz, A. J. *Am. Chem. Soc.* **2005**, *127*, 1596–1597. (c) Walensky, L. D.; Kung, A. L.; Escher, I.; Malia, T. J.; Barbuto, S.; Wright, R. D.; Wagner, G.; Verdine, G. L.; Korsmeyer, S. J. *Science* **2004**, *305*, 1466–1470. (d) Wang, J.-L.; Zhang, Z.-J.; Choksi, S.; Shan, S.; Lu, Z.; Croce, C. M.; Alnemri, E. S.; Korsmeyer, S. J.; Huang, Z. *Cancer Res.* **2000**, *60*, 1498–1502.
- (14) Structural characterization of BH3/Bcl-x_L interactions: (a) Bak/Bcl-x_L: Sattler, M.; Liang, H.; Nettessheim, D.; Meadows, R. P.; Harlan, J. E.; Eberstadt, M.; Yoon, H. S.; Shuker, S. B.; Chang, B. S.; Minn, A. J.; Thompson, C. B.; Fesik, S. W. *Science* **1997**, *275*, 983–986. (b) Bad/Bcl-x_L: Petros, A. M.; Nettessheim, D. G.; Wang, Y.; Olejniczak, E. T.; Meadows, R. P.; Mack, J.; Swift, K.; Matayoshi, E. D.; Zhang, H.; Thompson, C. B.; Fesik, S. W. *Protein Sci.* **2000**, *9*, 2528–2534. (c) Bim/Bcl-x_L: Liu, X.; Dai, S.; Zhu, Y.; Marrack, P.; Kappler, J. W. *Immunity* **2003**, *19*, 341–352.
- (15) (a) Ernst, J. T.; Becerril, J.; Park, H. S.; Yin, H.; Hamilton, A. D. *Angew. Chem., Int. Ed.* **2003**, *42*, 535–539. (b) Yin, H.; Lee, G.-I.; Sedey, K. A.; Rodriguez, J. M.; Wang, H.-G.; Sebt, S. M.; Hamilton, A. D. *J. Am. Chem. Soc.* **2005**, *127*, 5463–5468. (c) Yin, H.; Lee, G.-I.; Sedey, K. A.; Kutzki, O.; Park, H. S.; Orner, B. P.; Ernst, J. T.; Wang, H.-G.; Sebt, S. M.; Hamilton, A. D. *J. Am. Chem. Soc.* **2005**, *127*, 10191–10196.
- (16) (a) Chen, L.; Willis, S. N.; Wei, A.; Smith, B. J.; Fletcher, J. I.; Hinds, M. G.; Colman, P. M.; Day, C. L.; Adams, J. M.; Huang, D. C. S. *Mol. Cell.* **2005**, *17*, 393–403. (b) Willis, S. N.; Chen, L.; Dewson, G.; Wei, A.; Naik, E.; Fletcher, J. I.; Adams, J. M.; Huang, D. C. S. *Genes Dev.* **2005**, *19*, 1294–1305. (c) Certo, M.; Moore, V. D. G.; Nishino, M.; Wei, G.; Korsmeyer, S.; Armstrong, S. A.; Letai, A. *Cancer Cell* **2006**, *9*, 351–365.

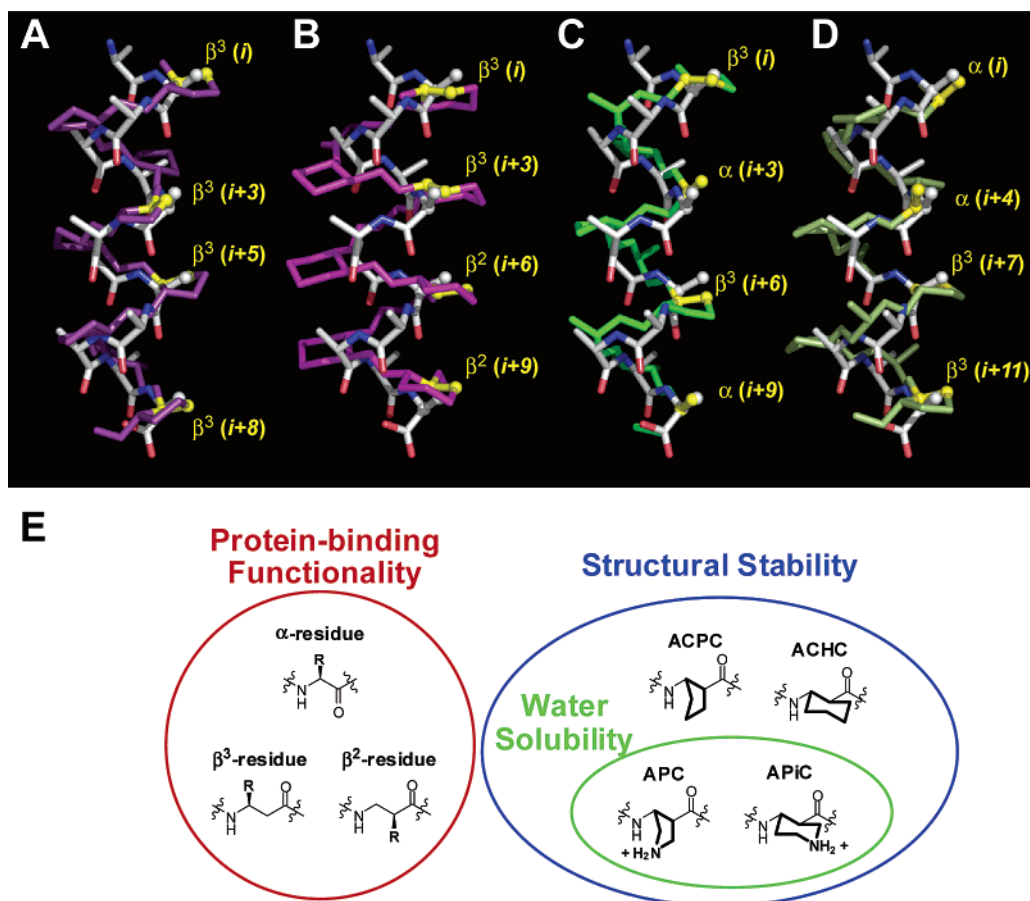


Figure 1. Framework for designing α -helix-mimetic β - and α/β -peptide foldamer ligands for protein surfaces. (A–D) Overlay of idealized foldamer helices (magenta/green) onto an idealized α -helix (colored by atom type). β -Peptides: (A) (ACPC)₉, 12-helix; (B) (ACHC)₁₀, 14-helix. α/β -Peptides: (C) (ACPC-Ala)₅, 11-helix; (D) (Ala-ACPC)₆, 14/15-helix. Foldamer structures from refs 8a and 17. Yellow bonds on foldamers indicate locations for side chains that align well with side chains *i*, *i* + 4, *i* + 7, and *i* + 11 (white ball-and-stick bonds) on the α -helix. (E) α -Amino acid and β -amino acid residue types used to endow α/β - or β -peptides with the chemical functionality (red), structural propensity (green and blue), and water solubility (green) central to our designs of α -helix-mimetic protein surface ligands.

Bcl-2, Bcl-w, A1, and Mcl-1.¹⁶ Thus, comparing affinities for unnatural ligands among these proteins would allow one to probe the selectivity of foldamer-protein recognition and ultimately learn how to control that selectivity. Insights acquired through the development of inhibitors within this family of helix-mediated protein recognition processes should provide a basis for efforts to block other types of protein–protein complexation in which α -helices play a prominent role, and perhaps also interactions that involve other types of surface topology.

The efforts described below stem from the exploration of two canonical foldamer classes, oligomers containing exclusively β -amino acid residues (“ β -peptides”) and oligomers with a 1:1 alternation of α - and β -amino acid residues (“ α/β -peptides”),⁸ as potential scaffolds for the development of α -helix-mimetic ligands for Bcl-x_L (Figure 1). Five distinct helices have been identified among β -peptides, and four among α/β -peptides.⁸ These helices are named on the basis of the characteristic backbone hydrogen-bonding patterns they contain; for example, the β -peptide 12-helix contains 12-membered ring C=O(*i*) → H–N(*i* + 3) H-bonds. The 12- and 14-helices are arguably the most fully characterized secondary structures among β -amino acid-containing foldamers.^{6,7,8e,17} Recent work suggests that the α/β -peptide 11- and 14/15-helices, too, are good platforms for design.^{8a,b} Each of these scaffolds generates a unique three-dimensional arrangement for a set of side chains with a given

sequence separation. A very simple molecular overlay analysis suggests that each of the four helices offers the possibility of spatially clustering proteinogenic side chains in a manner analogous to the side chain arrangement generated by an α -helical scaffold (Figure 1A–D).¹⁷ The helical conformations on which we focus can be strongly promoted by use of appropriate cyclically constrained β -amino acid residues (Figure 1E);⁸ the prospects of high shape stability and a straightforward way to vary this stability over a broad range are attractive design features. Seebach and co-workers have developed 14-helical β -peptide inhibitors of cholesterol absorption, a process dependent upon a specific α -helix-mediated protein–protein interaction.^{18a} More recently, the β -peptide 14-helix has been used by Schepartz et al. as a scaffold to develop ligands for the p53-binding cleft on hDM2.^{18b} In the p53–hDM2 complex

- (17) The structures of α/β - and β -peptide helices that could serve as α -helix-mimetic scaffolds are derived from high-resolution foldamer structures: (a) Appella, D. H.; Christianson, L. A.; Klein, D. A.; Powell, D. R.; Huang, X.; Barchi, J. J.; Gellman, S. H. *Nature* **1997**, *387*, 381–384. (b) Appella, D. H.; Christianson, L. A.; Karle, I. L.; Powell, D. R.; Gellman, S. H. *J. Am. Chem. Soc.* **1999**, *121*, 6206. See also ref 8a. (18) (a) Werder, M.; Hauser, H.; Abele, S.; Seebach, D. *Helv. Chim. Acta* **1999**, *82*, 1774–1783. (b) Kritzer, J. A.; Lear, J. D.; Hodsdon, M. E.; Schepartz, A. *J. Am. Chem. Soc.* **2004**, *126*, 9468–9469. (c) Stephens, O. M.; Kim, S.; Welch, B. D.; Hodsdon, M. E.; Kay, M. S.; Schepartz, A. *J. Am. Chem. Soc.* **2005**, *127*, 13126–13127. (d) English, E. P.; Chumanov, R. S.; Gellman, S. H.; Compton, T. *J. Biol. Chem.* **2006**, *281*, 2661–2667. (e) Sadowsky, J. D.; Schmitt, M. A.; Lee, H.-S.; Umezawa, N.; Wang, S.; Tomita, Y.; Gellman, S. H. *J. Am. Chem. Soc.* **2005**, *127*, 11966–11968.

itself, this cleft is occupied by an α -helical segment of p53.¹⁹ Another effort by this group has identified 14-helical β -peptides that interact with a protein that serves as a model for HIV protein gp41; these β -peptides block cell–cell fusion in a model for HIV infection.^{18c} We have discovered 12-helical β -peptides that inhibit cytomegalovirus infection of target cells,^{18d} a process that appears to depend upon α -helix coiled-coil interactions.²⁰ We have previously described preliminary efforts to identify and characterize foldameric ligands for the BH3-recognition cleft of Bcl-x_L based on α/β and β -peptides, which ultimately resulted in the discovery of potent ($\alpha/\beta+\alpha$)-peptide ligands (containing both an α/β and an α segment).^{18e} Below, we describe a multi-faceted approach to characterization of the most effective ligands, involving biophysical measurements of binding affinity, sequence–affinity relationships, and assays employing cell extracts.

Results

In the NMR-derived structure of the complex between Bcl-x_L and a 16-residue α -peptide from the Bak BH3 domain (Bak^{BH3}), Bak^{BH3} is bound as an amphipathic α -helix to a nonpolar cleft on Bcl-x_L.^{14a} Four hydrophobic side chains aligned along one face of the Bak^{BH3} helix, those of Val-74, Leu-78, Ile-81, and Ile-85 (residue numbering from the complete human Bak protein sequence), are buried in the Bak^{BH3}/Bcl-x_L interface and are energetically important for binding, as indicated by mutagenesis. Two charged side chains, those of Arg-76 and Asp-83, on the solvent-exposed face of the Bak^{BH3} α -helix are also important for binding, presumably because of electrostatic interactions with charged side chains on the periphery of the BH3-recognition cleft. The wealth of structural and binding data that has emerged since the structural elucidation of the Bak^{BH3}/Bcl-x_L complex has shown that the recognition cleft on Bcl-x_L (and related anti-apoptotic proteins) can accommodate other BH3 domains, for example, those from Bad and Bim, and that BH3 epitopes generally comprise a set of hydrophobic side chains aligned along one face of an α -helix and a few hydrophilic side chains on the opposite side of the helix.^{12,14b,c,16}

Preliminary Studies with Pure Foldamer Scaffolds. Our initial attempts to develop ligands for the BH3-recognition cleft of Bcl-x_L focused on the prospect that a natural α -helical ligand such as Bak^{BH3} could be mimicked in its entirety with a single foldamer scaffold. We started with β -peptide designs, and then expanded to α/β -peptide designs as sequence–structure relationships in this foldamer family were revealed.¹⁷ In each case, we sought to identify β - or α/β -peptide sequences that, in the predicted helical conformation, would project a set of side chains with appropriate physicochemical features (shape, hydrophobicity, and charge) in a spatial arrangement that mimics the set of six α -amino acid side chains composing the binding epitope of a BH3 domain.

To evaluate the affinity of foldamers for the BH3-recognition cleft of Bcl-x_L, we employed a competition fluorescence polarization (FP) assay, which measures the ability of compounds to inhibit the binding of a fluorophore-labeled BH3 peptide “probe” to Bcl-x_L (expressed as the IC₅₀, the concentration of inhibitor required for a 50% decrease in binding of the

probe). Initial FP assays employed a fluorescein-labeled peptide from the BH3 domain of Bak as the probe, as in previous studies.²¹ We found, however, that a BODIPY^{TMR}-labeled Bak^{BH3} peptide ($K_d = 4 \pm 1.9$ nM) displayed a ~ 10 -fold higher affinity for Bcl-x_L than did Flu-labeled Bak^{BH3} ($K_d = 39 \pm 4.2$ nM), permitting the design of a more sensitive competition FP assay.²² BODIPY^{TMR}-Bak^{BH3}, at 16 amino acid residues, shows comparable or higher affinity for Bcl-x_L relative to longer (20–25 residue) fluorescein-labeled BH3 peptides from other pro-apoptotic proteins (e.g., Bad and Bim).^{16c} In addition, common FP assay interferences arising from light scattering or fluorescent impurities are suppressed in assays that employ probes labeled with red-shifted fluorophores (e.g., BODIPY^{TMR}) relative to assays that employ fluorescein-labeled probes.²³ For these reasons, we used exclusively competition FP assays employing the BODIPY^{TMR}-Bak^{BH3} probe for the studies described here.

Competition FP analysis of >200 candidates revealed no high- or medium-potency inhibitors of the BODIPY^{TMR}-Bak^{BH3}/Bcl-x_L interaction (which we define here as having IC₅₀ values of <1 μ M or 1–50 μ M, respectively) among β -peptides designed to adopt a 12- or 14-helical conformation or among α/β -peptides designed to adopt an 11-helical conformation (oligomers 1–3 are representative; Figure 2). These findings reveal the limitations of simple overlay modeling of the type illustrated in Figure 1. Among several dozen α/β -peptides designed to adopt a 14/15-helical conformation, however, medium-affinity ligands were identified. Of these, 4 displayed the lowest IC₅₀ value, 35 μ M (Figure 2). IC₅₀ values are often converted to apparent dissociation constants (K_i) for inhibitor binding; a standard computational method gives $K_i = 4.2$ μ M for 4,²⁴ which is comparable to K_i values reported for most small-molecule ligands described for Bcl-x_L.¹¹

Chimeric Ligand Design. The affinity for Bcl-x_L of our tightest-binding foldamer with a “pure” backbone, 14/15-helical α/β -peptide 4, is ~ 50 -fold weaker than the affinity of the Bak^{BH3} α -peptide (IC₅₀ = 35 μ M vs 0.73 μ M; $K_i = 4.2$ μ M vs 0.087 μ M). By converting K_i to Gibbs free energy of inhibition ($\Delta G_i = -RT \ln(K_i)$; $T = 298$ K), we can estimate that 4 binds to Bcl-x_L less favorably than does Bak^{BH3} by ~ 2.3 kcal/mol. This comparison suggests that α/β -peptide 4 does not complement the BH3-recognition cleft of Bcl-x_L as well as does an appropriate α -peptide ligand such as Bak^{BH3}. We envisioned two potential explanations for this observation. One hypothesis is that the 14/15-helical scaffold is globally unsuited for effective mimicry of the side chain display provided by BH3 domain α -peptides in the bound conformations. An alternative hypothesis is that α/β -peptide affinity is limited because of an incongruity between only a portion of the 14/15-helical scaffold and a corresponding portion of the BH3-recognition cleft. To

(19) Kussie, P. H.; Gorina, S.; Marechal, V.; Elenbaas, B.; Moreau, J.; Levine, A. J.; Pavletich, N. P. *Science* **1996**, *274*, 948–953.

(20) Lopper, M.; Compton, T. J. *Virol.* **2004**, *78*, 8333–8341.

(21) Zhang, H.; Nimmer, P.; Rosenberg, S. H.; Ng, S.; Joseph, M. *Anal. Biochem.* **2002**, *307*, 70–75.

(22) The sensitivity of competition FP assays to weakly binding compounds is dependent upon the binding affinity of the fluorescent probe for the protein target. For example, see: Nikolovska-Coleska, Z.; Wang, R.; Fang, X.; Pan, H.; Tomita, Y.; Li, P.; Roller, P. P.; Krajewski, K.; Saito, N. G.; Stuckey, J. A.; Wang, S. *Anal. Biochem.* **2004**, *332*, 261.

(23) (a) Owicki, J. C. *J. Biomol. Screen.* **2000**, *5*, 297. (b) Banks, P.; Gosselin, M.; Prystay, L. *J. Biomol. Screen.* **2000**, *5*, 329. (c) Turek-Etienne, T. C.; Small, E. C.; Soh, S. C.; Xin, T. A.; Gaitonde, P. V.; Barrabee, E. B.; Hart, R. F.; Bryant, R. W. *J. Biomol. Screen.* **2003**, *8*, 176–184.

(24) For calculation of inhibitor binding dissociation constant (K_i) values from FP-derived IC₅₀ values, we used the following internet-based tool: Wang, R.; Nikolovska-Coleska, Z.; Fang, X.; Wang, S. The K_i Calculator. http://sw16.im.med.umich.edu/software/calc_ki/. Parameters: K_d for BODIPY^{TMR}-Bak^{BH3} = 4 nM, [BODIPY^{TMR}-Bak^{BH3}] = 33 nM, [Bcl-x_L] = 20 nM.

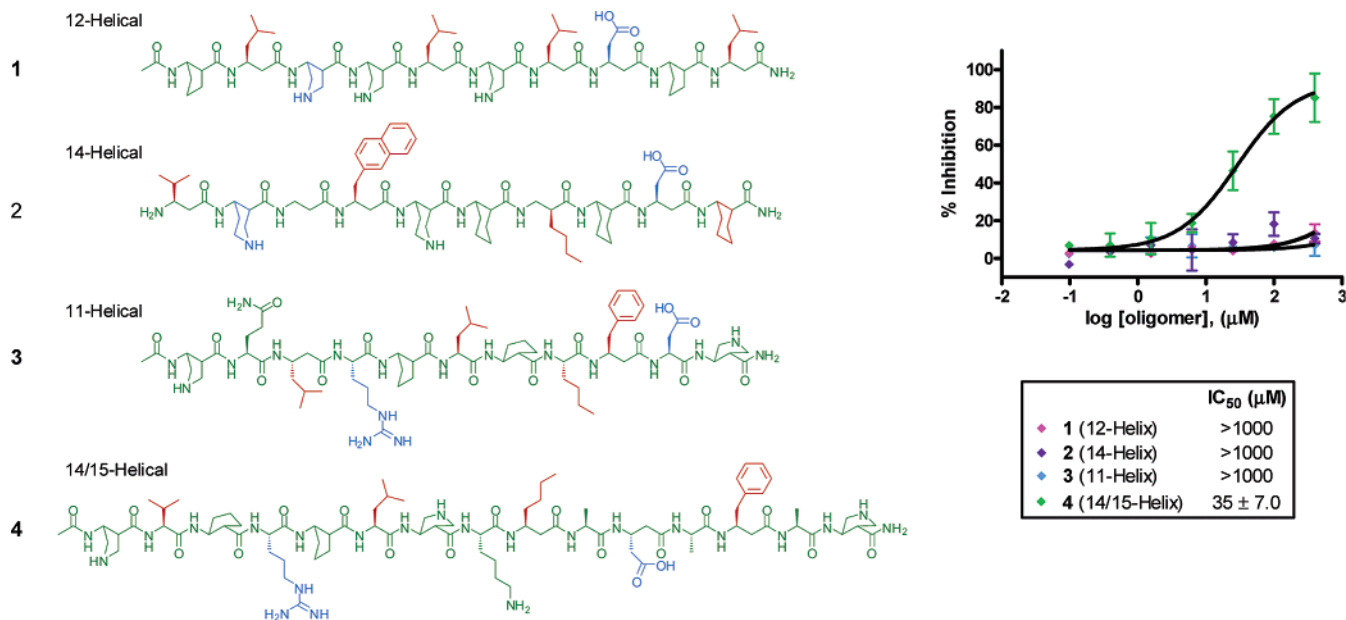


Figure 2. Structures and competition FP data for α/β - and β -peptide Bcl-x_L ligands 1–4. Oligomers shown represent one example of several dozen oligomers in each foldamer class. Side chains on 1–4 intended to mimic key side chains on a BH3 domain are indicated: red = hydrophobic, blue = charged. IC₅₀ values calculated from nonlinear curve-fitting in GraphPad Prism 4.0.

test the latter hypothesis, we devised a modified approach to ligand design that allowed us to target one part of the BH3-recognition cleft on Bcl-x_L with an α/β -peptide segment and the remaining part of the cleft with an α -peptide segment, that is, an approach based on chimeric oligomers.

The BH3-recognition site on Bcl-x_L can be divided conceptually into four hydrophobic pockets, each enveloping one of the four key hydrophobic side chains on an α -helical BH3 domain, and two charged regions, each forming electrostatic interactions with complementary charged side chains on a BH3 domain.¹⁴ Instead of trying to design a 14/15-helical α/β -peptide that interacts with all six contact points on Bcl-x_L simultaneously, we sought to target a subset of these contact points with an α/β -peptide segment, and thereby identify regions of the Bcl-x_L surface that might be complementary to this foldamer scaffold. We did not expect that short α/β -peptides would bind with measurable affinity to Bcl-x_L, given that such molecules would likely form only a few of the critical protein contacts seen in BH3/Bcl-x_L complexes.¹⁴ We therefore employed chimeric oligomers: short BH3-derived α -peptide segments that form part of the Bcl-x_L-binding surface were joined to α/β -peptide segments designed to make the remaining protein contacts (Figure 3A). Any difference in binding affinity (as indicated by IC₅₀ from the competition FP assay) between the full-length chimeric molecule and the α -peptide segment alone could be interpreted to indicate the extent to which the α/β -peptide fragment is complementary to the targeted region of the BH3-recognition surface on Bcl-x_L. This chimeric strategy bears some resemblance to fragment-based^{25,26} and ligand-extension²⁷ strategies, in which weakly binding molecular fragments are covalently linked to generate more potent ligands. However, our approach to Bcl-x_L ligand design differs from

these precedents in that we have focused on the rational design of foldamer fragments intended to mimic directly the secondary structure and side chain display of an α -helical protein fragment.

Our approach to developing chimeric Bcl-x_L ligands is illustrated in Figure 3 with a design in which a 14/15-helical α/β -peptide segment is fused to an α -peptide segment to generate an oligomer that we designate an ($\alpha/\beta+\alpha$)-peptide. This ($\alpha/\beta+\alpha$) design employs a 14/15-helical segment that is intended to present four of the six key BH3 domain side chains (Figure 3A). Specifically, the cluster of side chains displayed by α -amino acid residues at positions 2, 4, 6, and 9 in the 14/15-helical α/β -peptide fragment is intended to mimic the side chain cluster displayed by key Bak^{BH3} residues Val-74, Arg-76, Leu-78, and Ile-81, respectively. Residues 10–15 in the ($\alpha/\beta+\alpha$) chimera constitute an α -residue segment derived from a high-affinity α -peptide ligand for Bcl-x_L. Selection of the key side chains in chimeric ($\alpha/\beta+\alpha$)-peptides was guided by our mutational studies on the Bak^{BH3} α -peptide itself, which suggested that affinity could be improved via modification of side chains forming the hydrophobic face of the Bak^{BH3} helix that contacts Bcl-x_L.²⁸ For example, Bak^{BH3} analogue **5** (Figure 4) is the result of mutating the wild-type Bak^{BH3} sequence at four positions, three of which form part of the binding epitope (Val-74 → Leu, Ile-81 → Nle, and Ile-85 → Phe; Nle = norleucine) and the fourth of which does not contact Bcl-x_L (Asp-84 → Ala).¹⁵ α -Peptide **5** (IC₅₀ ≤ 0.013 μM; K_i ≤ 0.0002 μM) shows at least 400-fold greater affinity for Bcl-x_L than does wild-type Bak^{BH3} (K_i = 0.087 μM) in our FP assay. Side chains from **5** were incorporated into the N-terminal α/β

(25) Shuker, S. B.; Hajduk, P. J.; Meadows, R. P.; Fesik, S. W. *Science* **1996**, *274*, 1531–1534.

(26) (a) Zartler, E. R.; Shapiro, M. J. *Curr. Opin. Chem. Biol.* **2005**, *9*, 366–370. (b) Erlanson, D. A.; Hansen, S. K. *Curr. Opin. Chem. Biol.* **2004**, *8*, 399–406.

(27) (a) Kapoor, T. M.; Andreotti, A. H.; Schreiber, S. L. *J. Am. Chem. Soc.* **1998**, *120*, 23–29. (b) Morken, J. P.; Kapoor, T. M.; Feng, S.; Shirai, F.; Schreiber, S. L. *J. Am. Chem. Soc.* **1998**, *120*, 30–36. (c) Ferrer, M.; Kapoor, T. M.; Strassmaier, T.; Weissenhorn, W.; Skehel, J. J.; Oprian, D.; Schreiber, S. L.; Wiley, D. C.; Harrison, S. C. *Nat. Struct. Biol.* **1999**, *6*, 953–960. (d) Reddy, M. M.; Bachhawat-Sikder, K.; Kodadek, T. *Chem. Biol.* **2004**, *11*, 1127–1137.

(28) Sadowsky, J. D.; Peterson, K. J.; Tomita, Y.; Gellman, S. H., manuscript in preparation.

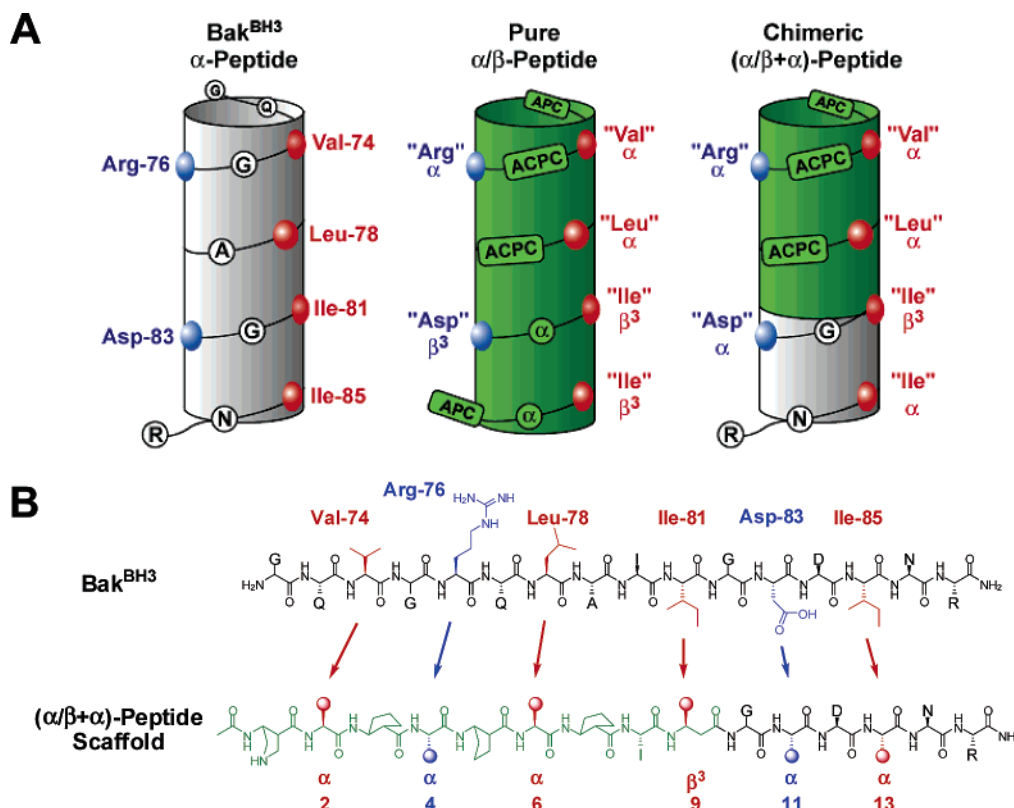


Figure 3. Chimeric approach to foldameric Bcl-x_L ligand design and comparison to an approach based on “pure” foldamers. (A) Schematic indicating mimicry of the entire Bak^{BH3} helix (gray cylinder) with a 14/15-helical α/β scaffold (green cylinder) or mimicry of a portion of Bak^{BH3} with a 14/15-helical α/β scaffold to generate a chimeric ($\alpha/\beta+\alpha$)-peptide (green/gray cylinder). (B) Mapping of the six key side chains in Bak^{BH3} (hydrophobic, red; charged, blue) onto a chimeric ($\alpha/\beta+\alpha$)-peptide scaffold.

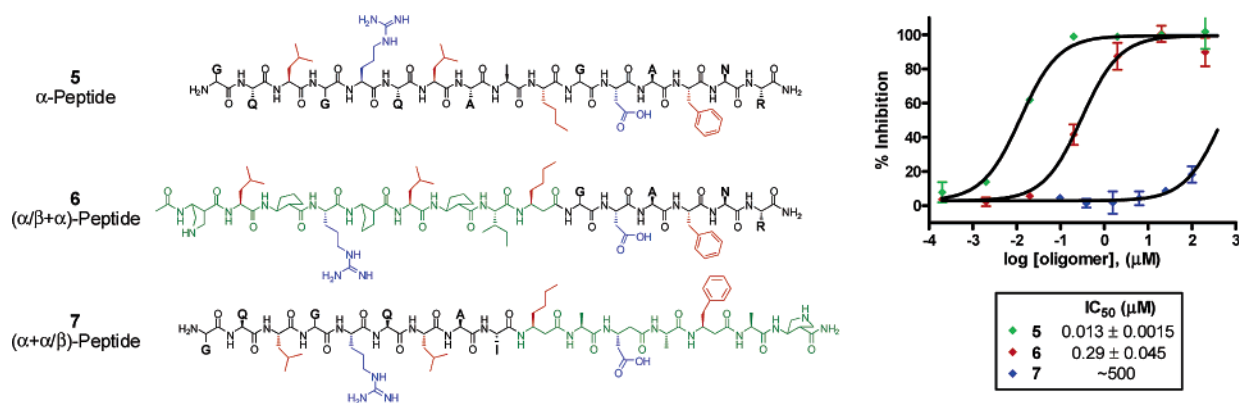


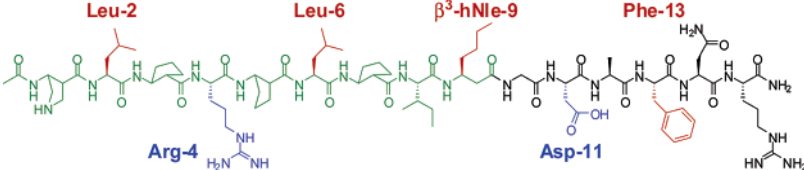
Figure 4. Structures and competition FP analysis of α -peptide Bak^{BH3} mutant **5**, ($\alpha/\beta+\alpha$)-peptide **6**, and ($\alpha+\alpha/\beta$)-peptide **7**. Hydrophobic and charged side chains on **6** and **7** intended to mimic analogous side chains on **5** are indicated in red and blue, respectively; other side chains in α portions are labeled with the one-letter code corresponding to the amino acid. IC₅₀ values calculated from nonlinear curve-fitting in GraphPad Prism 4.0.

segment of chimeric oligomer **6**, while the C-terminal α -residue segment was taken entirely from α -peptide **5** (Figure 4). The N-terminal portion of **6** contains cyclic β -amino acid residues (ACPC or APC) to promote helicity in the foldamer fragment and to impart water solubility (Figure 1E).

($\alpha/\beta+\alpha$)-Peptide **6** showed an FP-derived IC₅₀ value of 0.29 μ M ($K_i = 0.034 \mu$ M), a >100-fold improvement relative to our most active α/β -peptide, **4** ($\Delta\Delta G_i = -2.9$ kcal/mol). The α segment of **6** is not the only source of affinity because no binding to Bcl-x_L was detected via FP for the six-residue α -peptide corresponding to this segment (IC₅₀ > 1000 μ M, $K_i > 122 \mu$ M). Therefore, we conclude that the α/β segment of **6** contributes significantly to affinity for Bcl-x_L, presumably by making contacts with Bcl-x_L that mimic those made by the

N-terminal portion of Bak^{BH3} or α -peptide **5**. Alternative chimeric designs, such as ($\alpha+\alpha/\beta$)-peptide **7**, in which the N-terminal portion is derived from α -peptide **5** and the C-terminal portion is an α/β segment designed to mimic key side chains in the C-terminal portion of **5**, displayed little or no binding to Bcl-x_L (IC₅₀ \approx 500 μ M for **7**). Such findings strengthen our hypothesis that the 14/15-helical α/β -peptide scaffold can effectively mimic an α -helical BH3 ligand in one portion of the Bcl-x_L cleft but not the other. We examined chimeric designs analogous to **6** in which the N-terminal segment was designed to adopt a 12-helix ($(\beta+\alpha)$ oligomers) or an 11-helix ($(\alpha/\beta+\alpha)$ oligomers), but little or no binding to Bcl-x_L was observed in these cases (IC₅₀ > 500 μ M, not shown). These results are consistent with those obtained from analysis

Table 1. Alanine Scan of ($\alpha/\beta+\alpha$)-Peptide 6

entry	sequence	IC ₅₀ ± CI (K _i), μM ^a
6		0.29 ± 0.045 (0.034)
8	Ac-APC-Leu-ACPC-Arg-ACPC-Leu-ACPC-Ile-β ³ hNle-Gly-Asp-Ala-Phe-Asn-Arg-NH ₂	0.15 ± 0.025 (0.016)
9	Ac-APC-Leu-β ³ hAla-Arg-ACPC-Leu-ACPC-Ile-β ³ hNle-Gly-Asp-Ala-Phe-Asn-Arg-NH ₂	0.75 ± 0.095 (0.090)
10	Ac-APC-Leu-ACPC-Ala-ACPC-Leu-ACPC-Ile-β ³ hNle-Gly-Asp-Ala-Phe-Asn-Arg-NH ₂	6.6 ± 0.70 (0.80) ^b
11	Ac-APC-Leu-ACPC-Arg-β ³ hAla-Leu-ACPC-Ile-β ³ hNle-Gly-Asp-Ala-Phe-Asn-Arg-NH ₂	0.86 ± 0.085 (0.10) ^b
12	Ac-APC-Leu-ACPC-Arg-ACPC-Ala-ACPC-Ile-β ³ hNle-Gly-Asp-Ala-Phe-Asn-Arg-NH ₂	11 ± 5.9 (1.4)
13	Ac-APC-Leu-ACPC-Arg-ACPC-Leu-β ³ hAla-Ile-β ³ hNle-Gly-Asp-Ala-Phe-Asn-Arg-NH ₂	1.0 ± 0.12 (0.12)
14	Ac-APC-Leu-ACPC-Arg-ACPC-Leu-ACPC-Ala-β ³ hNle-Gly-Asp-Ala-Phe-Asn-Arg-NH ₂	0.13 ± 0.025 (0.014)
15	Ac-APC-Leu-ACPC-Arg-ACPC-Leu-ACPC-Ile-β ³ hAla-Gly-Asp-Ala-Phe-Asn-Arg-NH ₂	0.46 ± 0.050 (0.055)
16	Ac-APC-Leu-ACPC-Arg-ACPC-Leu-ACPC-Ile-β ³ hNle-Gly-Ala-Ala-Phe-Asn-Arg-NH ₂	11 ± 3.2 (1.3) ^b
17	Ac-APC-Leu-ACPC-Arg-ACPC-Leu-ACPC-Ile-β ³ hNle-Gly-Asp-Ala-Ala-Asn-Arg-NH ₂	38 ± 8.0 (4.6)
18	Ac-APC-Leu-ACPC-Arg-ACPC-Leu-ACPC-Ile-β ³ hNle-Gly-Asp-Ala-Phe-Ala-Arg-NH ₂	1.2 ± 0.21 (0.14)
19	Ac-APC-Leu-ACPC-Arg-ACPC-Leu-ACPC-Ile-β ³ hNle-Gly-Asp-Ala-Phe-Asn-Ala-NH ₂	5.4 ± 0.85 (0.65)

^a IC₅₀ and CI (95% confidence interval) calculated from curve-fitting in GraphPad Prism 4.0. K_i values calculated from IC₅₀ according to ref 24. ^b Showed FP behavior consistent with aggregation above 20 μM; IC₅₀ value is approximate. ACPC = *trans*-(1*S*,2*S*)-2-aminocyclopentancarboxylic acid; APC = *trans*-(3*S*,4*R*)-3-aminopyrrolidine-4-carboxylic acid; hNle = (*S*)-homonorleucine; hAla = (*S*)-homoalanine.

of pure foldamer ligand candidates (Figure 2) in suggesting that the 14/15-helix is more compatible than are other α/β - or β -peptide helices with at least a portion of the Bcl-x_L BH3-recognition cleft.^{18e}

Alanine Scanning. The side chains of six residues in ($\alpha/\beta+\alpha$)-peptide 6, Leu-2, Arg-4, Leu-6, β³-hNle-9, Asp-11, and Phe-13, were intended to form key contacts with the surface of Bcl-x_L, by analogy to the side chains of residues in Bak^{BH3} (Val-74, Arg-76, Leu-78, Ile-81, Asp-83, and Ile-85) and α -peptide 5 (Leu-74, Arg-76, Leu-78, Nle-81, Asp-83, and Phe-85) (Figure 3). To test this design hypothesis, we prepared a series of analogues of 6 in which each side chain was systematically replaced with a methyl group (i.e., α -residues, one at a time, were replaced by Ala, and β -residues were replaced by β³-homoalanine (β³-hAla)). Alanine scanning mutagenesis has been used extensively for identifying side chains that make energetically important contacts in protein–protein and peptide–protein interfaces (“hot-spot” residues).²⁹ A decrease in binding affinity due to replacement of a residue by alanine is generally interpreted to suggest that the deleted side chain engages in a favorable interaction with the complementary protein surface.

Large effects on binding were observed for alanine mutation of four out of six residues that were intended to form the Bcl-x_L-binding surface of 6: Arg-4 and Leu-6 in the α/β segment, and Asp-11 and Phe-13 in the α segment (Table 1 and Figure 5A). These mutations increased IC₅₀ in the competition FP assay by 23- to 130-fold relative to unmodified 6 ($\Delta\Delta G_i = +1$ to $+3$ kcal/mol; 10, 12, 16, and 17; Table 1). Thus, the side chains of Arg-4, Leu-6, Asp-11, and Phe-13 appear to form energetically important contacts with the surface of Bcl-x_L, possibly by mimicking key residues Arg-76, Leu-78, Asp-83, and Phe-85, respectively, in α -peptide 5. In contrast, alanine mutations of Leu-2 and β³-hNle-9 in the α/β portion of 6, designed to mimic key residues Leu-74 and Nle-81 in α -peptide 5, did not significantly increase IC₅₀ relative to 6 itself (8 and 15; Table

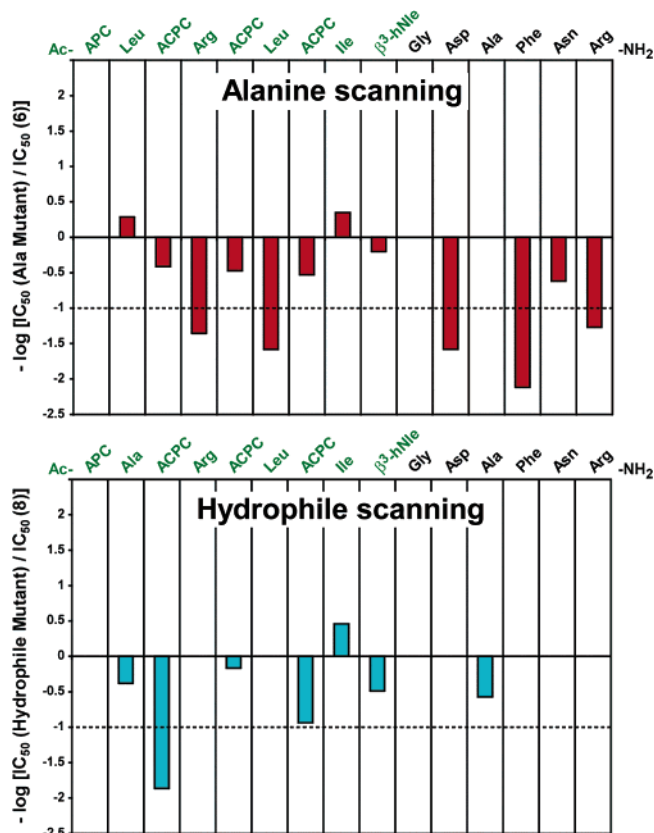
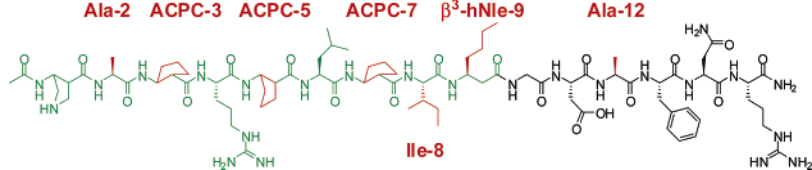


Figure 5. Comparison of hydrophile and alanine scanning results. (Top) Alanine scan data for ($\alpha/\beta+\alpha$)-peptide 6 from Table 1. (Bottom) Hydrophile scan data for ($\alpha/\beta+\alpha$)-peptide 8 from Table 2. Results are plotted as the negative logarithm of the ratio of IC₅₀ values for the oligomer with the alanine or hydrophilic mutation at the indicated sequence position and the unmodified oligomer, 6 or 8, respectively. Negative values indicate that the mutation decreased affinity for Bcl-x_L relative to 6 or 8. Dotted line marks a 10-fold relative increase in IC₅₀ value (decrease in affinity). No bar indicates a mutation that was not performed in these studies.

(29) (a) Clackson, T.; Wells, J. A. *Science* **1995**, *267*, 383–386. (b) DeLano, W. L. *Curr. Opin. Struct. Biol.* **2002**, *12*, 14–20.

1), implying that the side chains of these residues do not make energetically important contacts with the Bcl-x_L surface. In fact,

Table 2. Hydrophile Scan of ($\alpha/\beta+\alpha$)-Peptide **8**

entry	sequence	IC ₅₀ ± CI (K _i), μ M ^a
8	 Ala-2 ACPC-3 ACPC-5 ACPC-7 β^3 -hNle-9 Ala-12 Ile-8	0.15 ± 0.025 (0.016)
20	Ac-APC-Ala-ACPC-Arg-ACPC-Leu-ACPC-Ile- β^3 hNle-Gly-Asp-Ala-Phe-Asn-Arg-NH ₂	11 ± 2.3 (1.3)
21	Ac-APC-Ala-ACPC-Arg-APC-Leu-ACPC-Ile- β^3 hNle-Gly-Asp-Ala-Phe-Asn-Arg-NH ₂	0.22 ± 0.035 (0.025)
22	Ac-APC-Ala-ACPC-Arg-ACPC-Leu-APC-Ile- β^3 hNle-Gly-Asp-Ala-Phe-Asn-Arg-NH ₂	1.3 ± 0.47 (0.16)
23	Ac-APC-Lys-ACPC-Arg-ACPC-Leu-ACPC-Ile- β^3 hNle-Gly-Asp-Ala-Phe-Asn-Arg-NH ₂	0.36 ± 0.050 (0.043)
24	Ac-APC-Ala-ACPC-Arg-ACPC-Leu-ACPC-Lys- β^3 hNle-Gly-Asp-Ala-Phe-Asn-Arg-NH ₂	0.052 ± 0.0080 (0.005)
25	Ac-APC-Ala-ACPC-Arg-ACPC-Leu-ACPC-Ile- β^3 hLys-Gly-Asp-Ala-Phe-Asn-Arg-NH ₂	0.46 ± 0.050 (0.055)
26	Ac-APC-Ala-ACPC-Arg-ACPC-Leu-ACPC-Ile- β^3 hNle-Gly-Asp-Lys-Phe-Asn-Arg-NH ₂	0.56 ± 0.040 (0.067)

^a IC₅₀ and CI (95% confidence interval) calculated from curve-fitting in GraphPad Prism 4.0. K_i values calculated from IC₅₀ according to ref 24. ACPC, APC, and hNle are defined in Table 1. hLys = (S)-homolysine.

the small IC₅₀ decrease observed for the Leu-2 → Ala mutant, **8**, relative to **6** may indicate an unfavorable clash between the Leu-2 side chain of **6** and the surface of Bcl-x_L.

For most of the residues in ($\alpha/\beta+\alpha$)-peptide **6** that were not intended to mimic key contact residues of α -peptide **5**, mutation to Ala or β^3 -hAla had only a modest effect on IC₅₀ (<5-fold), suggesting that these deleted side chains may not make energetically important contacts with Bcl-x_L. An exception is the Arg-15 → Ala mutation (**19**; Table 1), which resulted in a 19-fold increase in IC₅₀, relative to **6** ($\Delta\Delta G_i = +1.8$ kcal/mol). The hydrocarbon portion of the Arg-87 side chain in wild-type Bak^{BH3}, analogous to Arg-15 in **6**, is in van der Waals contact with Bcl-x_L Leu-194 in the Bak^{BH3}/Bcl-x_L complex, and the Bak^{BH3} Arg-87 guanidinium group is proximal to the carboxylate of Bcl-x_L Glu-193.^{14a} On the basis of these contacts in the Bak^{BH3}/Bcl-x_L complex, we suspect that mutation of Arg-15 in **6** to Ala may remove hydrophobic and/or electrostatic contacts that stabilize binding to Bcl-x_L.

Hydrophile Scanning. The high affinity of ($\alpha/\beta+\alpha$)-peptide **6** for Bcl-x_L is intriguing in light of the alanine scanning results (Table 1, Figure 5A), which suggest that only four out of six intended “hot-spot” residues in **6** make energetically important contacts with Bcl-x_L. As mentioned above, Bak^{BH3} makes six important contacts with the surface of Bcl-x_L,^{14a} but the Bak^{BH3} peptide binds ~3-fold less strongly to Bcl-x_L than does **6**. We wondered whether other hydrophobic side chains on **6** not originally intended to contribute to the binding surface, for example, the cyclopentane rings of ACPC residues, are buried upon association with Bcl-x_L. Each replacement of an ACPC residue in **6** with β^3 -hAla was observed to cause an IC₅₀ increase of ~3-fold ($\Delta\Delta G_{\text{binding}} \approx 0.7$ kcal/mol; **9**, **11**, and **13**; Table 1), suggesting only a modest contribution by the side chain of each of these residues to Bcl-x_L affinity. The origin of these effects is unclear, however, because the ACPC → β^3 -hAla mutation alters both side chain shape and local backbone flexibility (due to removal of the ring constraint).

In an effort to gain further insight regarding which nonpolar side chains on an ($\alpha/\beta+\alpha$)-peptide ligand are buried upon complexation to Bcl-x_L, we carried out a “hydrophile scan”, in which nonpolar side chains are systematically replaced with a hydrophilic (e.g., cationic) analogue. If hydrophobic residues are buried in the hydrophobic cleft of Bcl-x_L, their substitution

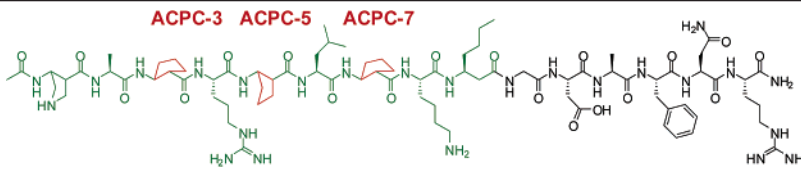
by charged residues should result in decreased binding affinity because of unfavorable desolvation upon burial of the charged group at the nonpolar interface.³⁰ In addition to providing useful structural information, hydrophile scanning offers the benefit of systematically identifying positions in oligomeric ligands at which side chains that promote aqueous solubility can be incorporated without diminishing binding affinity for a protein target. The hydrophile scan studies (Table 2 and Figure 5B) were based on ($\alpha/\beta+\alpha$)-peptide **8** (the Leu-2 → Ala mutant of **6**), which displays somewhat higher affinity for Bcl-x_L relative to **6** (Table 1).

Replacement of ACPC-3 or ACPC-7 in ($\alpha/\beta+\alpha$) oligomer **8** with APC resulted in a 74- or 9-fold increase in IC₅₀ in the FP assay (i.e., a decrease in affinity for Bcl-x_L of 2.6 or 1.3 kcal/mol, respectively), while the ACPC-5 → APC substitution had a negligible effect ($\Delta\Delta G_i \approx +0.2$ kcal/mol for **21** relative to **8**; Table 2). The five-membered rings of ACPC and APC are isosteric and impose similar constraints on the backbone of the α/β portion of **8**, but the APC pyrrolidine ring should bear a positive charge under our FP binding assay conditions (pH 7.4), while the ACPC cyclopentane ring is hydrophobic. Therefore, the substantial decrease in affinity observed upon replacing ACPC-3 or ACPC-7 in **8** with APC suggests that these residues become buried in the hydrophobic BH3-recognition cleft of Bcl-x_L upon binding. By contrast, ACPC-5 seems to project away from the interface. In light of these data, we conclude that the modest increase in IC₅₀ that results from replacing ACPC-5 in **6** with β^3 -hAla (Table 1, Figure 5A) reflects primarily an increase in backbone flexibility that this substitution should cause. The modest increase in IC₅₀ observed upon replacing ACPC-3 or ACPC-7 in **6** with β^3 -hAla (Table 1), on the other hand, may reflect counterbalancing effects of backbone flexibility and direct (favorable or unfavorable) contacts made by the side chains of these ACPC residues with the Bcl-x_L surface (see Discussion).

Hydrophobic → hydrophilic mutations of residues in **8** other than the three ACPC residues allowed us to explore whether other ($\alpha/\beta+\alpha$)-peptide side chains are buried in the interface and to improve the aqueous solubility of ($\alpha/\beta+\alpha$) ligands. The selection of an isosteric, hydrophilic, and synthetically accessible replacement for hydrophobic α or β^3 residues in **8** is not as

(30) Stites, W. E. *Chem. Rev.* **1997**, *97*, 1233–1250 and references therein.

Table 3. Backbone Mutations of ($\alpha/\beta+\alpha$)-Peptide **24**

entry	sequence	IC ₅₀ ± CI (K _i), μM ^a
24	 Ac-APC-Ala-ACPC-Arg-ACPC-Leu-ACPC-Lys-β ³ hNle-Gly-Asp-Ala-Phe-Asn-Arg-NH ₂	0.052 ± 0.0080 (0.005)
27	Ac-APC-Ala- ^{ent} ACPC-Arg-ACPC-Leu-ACPC-Lys-β ³ hNle-Gly-Asp-Ala-Phe-Asn-Arg-NH ₂	1.0 ± 0.20 (0.12)
28	Ac-APC-Ala-ACPC-Arg- ^{ent} ACPC-Leu-ACPC-Lys-β ³ hNle-Gly-Asp-Ala-Phe-Asn-Arg-NH ₂	68 ± 9.0 (8)
29	Ac-APC-Ala-ACPC-Arg-ACPC-Leu- ^{ent} ACPC-Lys-β ³ hNle-Gly-Asp-Ala-Phe-Asn-Arg-NH ₂	270 ± 30 (33)
30	Ac-APC-Ala-ACHC-Arg-ACPC-Leu-ACPC-Lys-β ³ hNle-Gly-Asp-Ala-Phe-Asn-Arg-NH ₂	0.16 ± 0.015 (0.018)
31	Ac-APC-Ala-ACPC-Arg-ACHC-Leu-ACPC-Lys-β ³ hNle-Gly-Asp-Ala-Phe-Asn-Arg-NH ₂	0.08 ± 0.013 (0.008)
32	Ac-APC-Ala-ACPC-Arg-ACPC-Leu-ACHC-Lys-β ³ hNle-Gly-Asp-Ala-Phe-Asn-Arg-NH ₂	0.19 ± 0.035 (0.021)

^a IC₅₀ and CI (95% confidence interval) calculated from curve-fitting in GraphPad Prism 4.0. K_i values calculated from IC₅₀ according to ref 24. ACPC, APC, and hNle defined in Table 1. ^{ent}ACPC = *trans*-(1*R*,2*R*)-2-aminocyclopentancarboxylic acid; ACHC = *trans*-(1*S*,2*S*)-2-aminocyclohexancarboxylic acid.

straightforward as the selection of APC for the replacement of ACPC. We chose to substitute acyclic, hydrophobic residues in **8** with Lys or β³-hLys; however, the methylene groups of the Lys side chain may form hydrophobic contacts with the surface of Bcl-x_L and thereby attenuate the deleterious effects of introducing the charged ammonium group into a hydrophobic cavity. Lys/β³-hLys substitutions were generally tolerated without large decreases in binding affinity (**23**–**26**; Table 2, Figure 5B). For example, Ala-2 → Lys and β³-hNle-9 → β³-hLys mutations (oligomers **23** and **25**, respectively) caused an increase in IC₅₀ by only 2.5- and 3.2-fold, respectively, suggesting that the side chains at these positions may not be extensively buried. These results correlate with those from the alanine scan, which suggest that side chains of residues 2 and 9 in **6** are not very important for binding to Bcl-x_L (Table 1, Figure 5A). Substituting Ile-8 in **8** for Lys (oligomer **24**) was actually favorable (IC₅₀ was decreased by ~2.5-fold), mirroring a similar effect on affinity observed upon substituting Ile-8 in **6** for Ala (**14**; Table 1). The β-branched side chain of Ile-8 in **6** and **8** may disfavor binding to Bcl-x_L relative to methyl (Ala) or aminobutyl (Lys) side chains by destabilizing helix formation in the ligand^{8b} and/or clashing with the surface of Bcl-x_L. Alternatively, formation of a helix-stabilizing electrostatic interaction between the side chains of Lys-8 and Asp-11 may explain increased binding of **24** relative to **8**; previous NMR structural analysis of ($\alpha/\beta+\alpha$)-peptide analogue **23** was consistent with the juxtaposition of residues 8 and 11 across one turn of a helix,^{18e} possibly poised for an electrostatic interaction. ($\alpha/\beta+\alpha$)-Peptide **24** represents an improvement in IC₅₀ of ~6-fold relative to **6**, and **24** has higher water solubility. The potency of **24** (K_i = 0.005 μM) is ~17-fold higher than that of the wild-type Bak^{BH3} α-peptide (K_i = 0.087 μM; ΔΔG_i = -1.7 kcal/mol)^{18e} and within ~5-fold of the potency of a 25-residue BH3 α-peptide from Bad (K_i = 0.0009 μM); the Bad 25-mer is one of the tightest-binding Bcl-x_L ligands in the literature.^{11,14b,16}

Backbone Perturbation Effects on Binding Affinity. An assumption behind the design of chimeric ($\alpha/\beta+\alpha$) foldamers is that these molecules, like BH3 α-peptides, adopt helical conformations when bound to Bcl-x_L. We have shown previously with 2D NMR measurements that ($\alpha/\beta+\alpha$)-peptide **23** (Table 2) in methanol adopts a hybrid helical conformation consisting of an N-terminal 14/15-helix formed by the α/β -peptide segment followed by a C-terminal α-helical turn formed

by the α-peptide segment.^{18e} By comparing the affinity of the β³-hNle-9 → β³-hLeu mutant of **24** (designated **4** in ref 18e and **33** in Figure 7) with that of its enantiomer (IC₅₀ = 0.029 μM vs >1000 μM, respectively), we demonstrated that only the right-handed ($\alpha/\beta+\alpha$)-peptide helix is effectively recognized by Bcl-x_L.^{18e} Here, we evaluate the effects of local conformational perturbations of the ($\alpha/\beta+\alpha$)-peptide backbone on affinity for Bcl-x_L.

Conformational perturbation studies focused on the α/β -peptide portion of **24** to enable us to evaluate the importance of 14/15-helical folding for binding to Bcl-x_L. Individual (*S,S*)-ACPC residues were replaced either with (*R,R*)-ACPC residues or with homologous six-membered-ring β-amino acid residues, (*S,S*)-ACHC (Figure 1E). Altering the absolute configuration of an ACPC inverts the preferred N-C_{β3}-C_{β2}-C backbone torsion angle (θ) from approximately +96° to -96° (based on crystal structures of ACPC homooligomers¹⁷) and should consequently prevent 14/15-helical folding. This substitution is analogous to replacing L-α-amino acid residues in α-peptides with D-residues, a strategy that has often been used to determine whether α-peptide folding is important for protein receptor binding.³¹ The replacement of five-membered-ring β-amino acid residues with six-membered-ring residues (5M → 6M substitutions) has the more subtle effect of shifting the preferred backbone N-C_{β3}-C_{β2}-C torsion angle from +96° to +56°.¹⁷

(*S,S*)-ACPC → (*R,R*)-ACPC mutants of **24** had 19- to 5200-fold higher IC₅₀ values relative to homochiral oligomer **24** in the competition FP assay (**27**–**29**; Table 3). Decreases in affinity for Bcl-x_L were largest for the two substitutions in the center of the sequence. Replacement of individual five-membered-ring residues in **24** with six-membered-ring residues resulted in smaller increases in IC₅₀ than did changing the configuration of individual ACPC residues (**30**–**32**; Table 3). Single 5M → 6M mutations increased IC₅₀ by <4-fold, implying that localized backbone perturbations of the α/β segment in **24** can be accommodated by the BH3-recognition cleft of Bcl-x_L. Overall, these results are consistent with our hypothesis that the α/β segment of peptide **24** must adopt a continuous helical conformation, presumably the 14/15-helix, to bind tightly to Bcl-x_L.

Docking Simulations and Correlation to Structure–Activity Relationships. We constructed a computational model

(31) For example: Grieco, P.; Balse, P. M.; Weinberg, D.; MacNeil, T.; Hruby, V. J. *J. Med. Chem.* **2000**, *43*, 4998–5002.

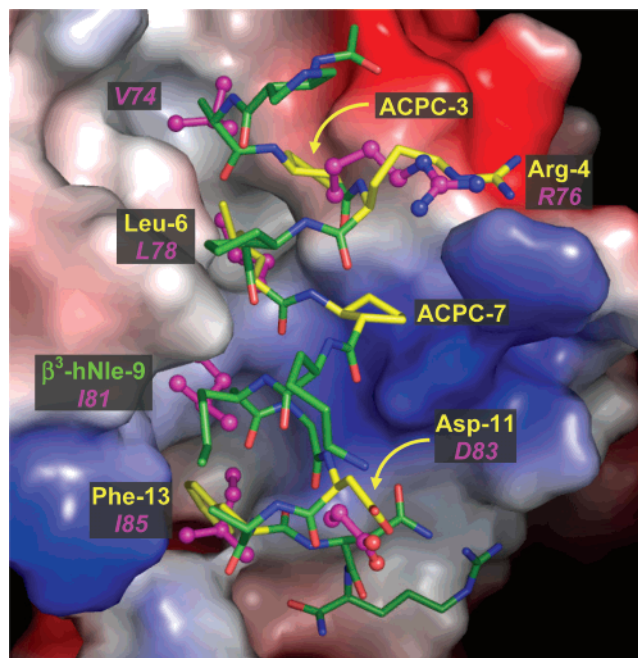


Figure 6. Computational model of ($\alpha/\beta+\alpha$)-peptide **24** bound to the BH3-recognition cleft of Bcl-x_L (surface). Side chains of residues in **24** that resulted in significant losses in Bcl-x_L affinity upon substitution with Ala (R4, L6, F13) or APC (ACPC-3, ACPC-7) are indicated in yellow; β^3 -hNle-9 is labeled in green. The key side chains of Bak^{BH3} are also shown and labeled (magenta, italics). Bcl-x_L surface is colored according to electrostatic potential. Figure was generated in PyMol.

of ($\alpha/\beta+\alpha$)-peptide **24** bound to the BH3-recognition cleft of Bcl-x_L in an effort to rationalize the sequence–affinity relationships presented above. To start, we generated a model of **24** in which the backbone conformation of the α/β portion was constrained to adopt a 14/15-helix and the backbone conformation of the α portion was constrained to mimic the backbone conformation of the analogous portion of Bak^{BH3} in its complex with Bcl-x_L. This structural model takes into account our previous NMR data that showed 14/15-helical folding of the N-terminal α/β portion of **23** (the Ala-2 → Lys/Lys-8 → Ile mutant of **24**).^{18c} The C-terminus of Bak^{BH3} in complex with Bcl-x_L deviates from ideal α -helicity.^{14a} On the basis of the sequence similarity in the C-termini of Bak^{BH3} and **24**, we assumed that the C-terminus of **24** will similarly deviate from α -helicity upon binding to Bcl-x_L. Oligomer **24** was docked into the Bcl-x_L cleft using Flexidock in Sybyl.³² All side chain torsional motions in **24** were permitted during docking calculations.

The lowest energy result of docking calculations (Figure 6) accounts for the sequence–affinity relationships established experimentally among ($\alpha/\beta+\alpha$)-peptides (Tables 1–3, Figure 5).³³ In the docked complex, the side chains of α -amino acid residues Arg-4, Leu-6, Asp-11, and Phe-13 of **24** complement regions of the Bcl-x_L surface occupied by side chains of key residues in Bak^{BH3}, Arg-76, Leu-78, Asp-83, and Ile-85,

(32) Such rigid-body docking calculations were not expected to be rigorous. It is known that peptide–protein docking calculations rarely predict structural data with high accuracy when receptor and ligand flexibility are not considered. However, given the empirical observations that an ($\alpha/\beta+\alpha$)-peptide analogue of **24**, compound **23**, is well-folded in methanol, that folding seems to be important for binding of **24** to Bcl-x_L, and that 40% of the sequence of **24** contains an α -peptide segment related to Bak^{BH3}, rigid docking of **24** in a helical conformation to the Bak^{BH3}-bound conformation of Bcl-x_L may be qualitatively predictive of the actual structure of the complex.

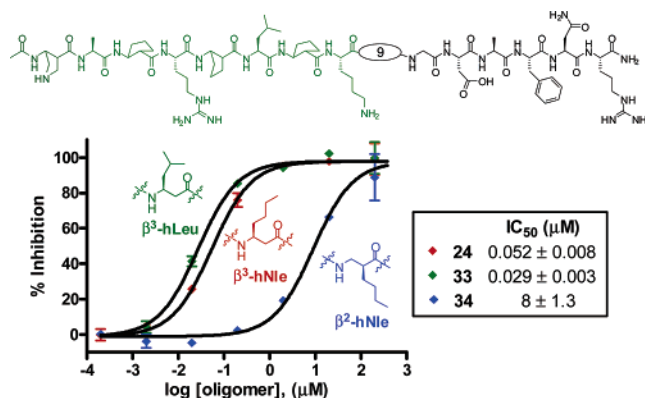


Figure 7. Sequence–affinity relationships for analogues of ($\alpha/\beta+\alpha$)-peptide **24** with substitutions at position 9 (oligomers **33** and **34**). Residues incorporated at position 9 are indicated on competition FP binding curves in color; IC₅₀ values calculated from curve-fitting are shown.

respectively. The side chains of Leu-6 and Phe-13 in **24** are deeply buried in the BH3-recognition cleft of Bcl-x_L, while Arg-4 and Asp-11 are close to complementary charged residues on the edges of the Bcl-x_L cleft. The hypothetical contacts made by residues 4, 6, 11, and 13 in **24** with the BH3 cleft are consistent with our observation that Ala mutations at these positions in ($\alpha/\beta+\alpha$) oligomer **6** caused large decreases in affinity for Bcl-x_L (Table 1, Figure 5A). The cyclopentyl side chains of ACPC-3 and ACPC-7, identified as buried in a hydrophobic environment by ACPC → APC mutation studies of analogue **8** (Table 2, Figure 5B), are buried in hydrophobic pockets in the BH3-recognition cleft of Bcl-x_L in docked **24**. The hydrophobic side chain of Ala-12 of **24**, in contrast, seems to make little or no contact with the Bcl-x_L surface, and the side chain of ACPC-5 makes contact with Bcl-x_L Phe-105, but is not extensively buried in the BH3-recognition cleft of Bcl-x_L. These features of the docking model are consistent with the observation that replacement of ACPC-5 or Ala-12 in **8** with a charged residue does not significantly reduce Bcl-x_L affinity (Table 2, Figure 5B).

The *n*-butyl side chain of β^3 -hNle-9 in **24** packs tightly against the hydrophobic surface of the BH3-binding cleft of Bcl-x_L in our hypothetical structure of the **24**/Bcl-x_L complex (Figure 6). This aspect of the computational model seems to be at odds with the experimental observation that the β^3 -hNle-9 → β^3 -hAla mutation in **6** has relatively little impact on affinity (Table 1), unless forming a favorable interaction between the *n*-butyl side chain of β^3 -hNle-9 and the Bcl-x_L surface requires a counteracting unfavorable steric or torsional adjustment in the ligand or protein. We examined the possibility of steric clashing between the β^3 -hNle side chain of **24** and Bcl-x_L empirically by evaluating additional modifications of the residue at position 9 (Figure 7). Changing the side chain shape via β^3 -hNle-9 → β^3 -hLeu mutation caused a slight but reproducible ~ 1.6 -fold

(33) The other low-energy docked complexes (defined as those having scoring energies within 4 kcal/mol of the lowest energy complex) did not differ greatly from the lowest-energy complex shown in Figure 6. We performed a second round of docking calculations starting with an orientation of **24** in the BH3-binding pocket of Bcl-x_L that was rotated $\sim 180^\circ$ (i.e., the positions of the N-terminus and C-terminus were swapped) relative to that shown in Figure 6. This experiment resulted in low-energy complexes that had scoring energies > 30 kcal/mol higher than complexes from the first round. All of the low-energy complexes from the second round, however, showed **24** oriented in the BH3-recognition cleft in a manner similar to that in Figure 6 (i.e., **24** had rotated $\sim 180^\circ$ back to the orientation found in the first round of docking), but side chain/Bcl-x_L contacts were diminished due to translation of the oligomer out of the Bcl-x_L cleft.

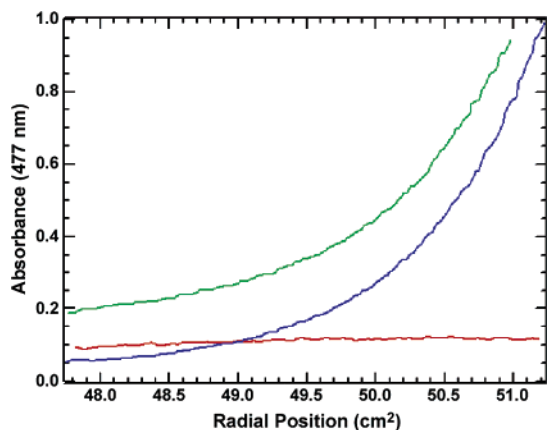


Figure 8. Analytical ultracentrifugation analysis of **Flu-Ahx-24** binding to Bcl-x_L. Ligand:protein concentration ratios = 6 μM:4 μM (green), 12 μM:4 μM (blue), and 6 μM:0 μM (red). Rotor speed for data shown was 30 000 rpm. Absorbance was monitored at 477 nm.

decrease in IC₅₀ (this analogue is designated **4** in ref 18e and **33** in Figure 7; IC₅₀ = 0.029 μM). This observation suggests that the isobutyl side chain of β³-hLeu is slightly more favorably accommodated by the Bcl-x_L surface than is the *n*-butyl side chain of β³-hNle. Replacing β³-hNle-9 with β²-hNle, which shifts the side chain by one C–C bond along the backbone, resulted in a >150-fold increase in IC₅₀ (8 μM for **34** vs 0.052 μM for **24**; ΔΔG_i = +3.1 kcal/mol). Simple extrapolation from the predicted structure of **24** bound to Bcl-x_L (Figure 6) suggests that the β³-hNle-9 → β²-hNle substitution would cause the *n*-butyl side chain to clash with the surface of Bcl-x_L.

Determination of Binding Stoichiometry. The FP-based studies outlined above indicate that (α/β+α)-peptide foldamers compete effectively with Bak^{BH3} for binding to Bcl-x_L. Thus, the FP results are consistent with a model in which these oligomers target the BH3-recognition cleft on Bcl-x_L. Alternative mechanisms of probe displacement in the FP assay are possible, however, including allosteric or multisite binding and ligand-induced unfolding of Bcl-x_L. An HSQC NMR binding experiment conducted with (α/β+α)-peptide **24** and ¹⁵N-labeled Bcl-x_L showed that this ligand caused numerous resonances in Bcl-x_L to shift upon binding,^{18e} a result that could reflect multisite binding; however, similarly extensive resonance shifts are observed upon binding of BH3 peptides (e.g., Bak^{BH3}, Bid^{BH3}, and Bad^{BH3}) to Bcl-x_L.^{13c,14a,b,18e,34} To examine the nature of (α/β+α)-peptide/Bcl-x_L binding further, we undertook analytical ultracentrifugation (AU) studies, which enabled determination of ligand/protein stoichiometry.

A fluorescein-labeled analogue of **24** was prepared to allow us to examine binding of the (α/β+α)-peptide to Bcl-x_L via AU by measuring absorbance at 477 nm. In **Flu-Ahx-24**, the Flu and (α/β+α)-peptide units are separated by an ε-amino-hexanoic acid (Ahx) spacer; **Flu-Ahx-24** binds tightly to Bcl-x_L, according to a titration FP assay (*K*_d = 0.0008 μM). Strong binding was qualitatively confirmed by sedimentation of **Flu-Ahx-24** to the bottom of the AU sample cell upon centrifugation at 30 000 rpm in the presence of Bcl-x_L, but not in the absence of the protein (Figure 8).

Protein–ligand binding stoichiometry is expected to show a pronounced dependence on environment;^{1a} therefore, we deter-

mined the **Flu-Ahx-24**/Bcl-x_L stoichiometry in two different buffers. The first set of AU studies was carried out in a medium generated by 8-fold dilution of the buffer used to store Bcl-x_L (phosphate-buffered saline (PBS) with 2 mM β-mercaptoethanol) into the buffer used for FP competition and direct-binding assays (PBS with 0.05% (w/v) Pluronic F-68 non-ionic detergent). The second set of AU studies was carried out in pure Bcl-x_L storage buffer (i.e., no added detergent). All AU samples contained 4% (v/v) DMSO from addition of **Flu-Ahx-24**. The **Flu-Ahx-24**/Bcl-x_L binding stoichiometry was determined by comparing UV absorbance of ligand at the meniscus of the AU cell (i.e., unbound ligand) for samples containing different **Flu-Ahx-24**:Bcl-x_L ratios: 6 μM:4 μM, 12 μM:4 μM, and 6 μM:0 μM.

In the detergent-containing buffer (also used for FP analysis), the **Flu-Ahx-24**/Bcl-x_L stoichiometry was calculated to be 1.0:1, which indicates that **Flu-Ahx-24** targets a single site on the surface of Bcl-x_L. This finding is consistent with our design goal that the (α/β+α)-peptide should mimic a natural BH3 domain and bind to the appropriate recognition cleft on Bcl-x_L. In the buffer lacking detergent, however, the **Flu-Ahx-24**/Bcl-x_L stoichiometry is 1.8:1, implying multisite binding (uncertainty in stoichiometry measurements is ~10%).³⁵ Our finding that 1:1 **Flu-Ahx-24**:Bcl-x_L binding requires the presence of a non-ionic detergent is consistent with the emerging view that molecules displaying substantial nonpolar surfaces (which include many protein-binding small molecules) can engage in unintended and undesirable hydrophobically driven interactions.^{1,36} It is possible that, in the absence of detergent, **Flu-Ahx-24** can interact with a second, unanticipated binding site on Bcl-x_L, or that **Flu-Ahx-24** can form small aggregates that interact with Bcl-x_L in a biologically irrelevant way. Evidence against the latter hypothesis includes our observation, by AU, that **Flu-Ahx-24** is, by itself, mostly or entirely monomeric (not shown). In any case, the observation of 1:1 binding stoichiometry in the presence of detergent indicates that under the conditions employed for FP competition experiments described above, binding of (α/β+α)-peptides to Bcl-x_L should involve a 1:1 stoichiometry. Therefore, sequence–affinity relationships for (α/β+α)-peptides derived from FP data can be interpreted in terms of binding to a single site on Bcl-x_L.

Several additional lines of evidence, beyond AU, support a single-site binding model for the interaction of (α/β+α)-peptides with Bcl-x_L in FP studies. Shoichet et al. have noted that aggregation of poorly soluble ligand molecules can give rise to spurious evidence for protein–ligand interactions, because such aggregates can display moderate but biologically irrelevant affinity for proteins.^{36a–c} The onset of this type of effect, however, is typically seen at micromolar ligand concentrations. The most potent (α/β+α)-peptide inhibitors described here, on the other hand, bind to Bcl-x_L at concentrations of 10–100 nM. Further evidence for discrete and specific binding of (α/β+α)-peptides to Bcl-x_L can be found in the sensitivity of FP-derived

(34) Lugovskoy, A. A.; Degterev, A. I.; Fahmy, A. F.; Zhou, P.; Gross, J. D.; Yuan, J.; Wagner, G. *J. Am. Chem. Soc.* **2002**, *124*, 1234–1240.

(35) The stoichiometry for the interaction of Flu-Bak^{BH3}, the wild-type Bak^{BH3} peptide labeled at the N-terminus with fluorescein, with Bcl-x_L was less sensitive to these buffer changes: Flu-Bak^{BH3}/Bcl-x_L stoichiometry was 0.7:1 in the detergent-containing buffer and 1.0:1 in buffer lacking detergent. (a) McGovern, S. L.; Caselli, E.; Grigorieff, N.; Shoichet, B. K. *J. Med. Chem.* **2002**, *45*, 1712–1722. (b) McGovern, S. L.; Helfand, B. T.; Feng, B.; Shoichet, B. K. *J. Med. Chem.* **2003**, *46*, 4265–4272. (c) Seidler, J.; McGovern, S. L.; Doman, T. N.; Shoichet, B. K. *J. Med. Chem.* **2003**, *46*, 4477–4486. (d) Ryan, A. J.; Gray, N. M.; Lowe, P. N.; Chung, C.-W. *J. Med. Chem.* **2003**, *46*, 3448–3451.

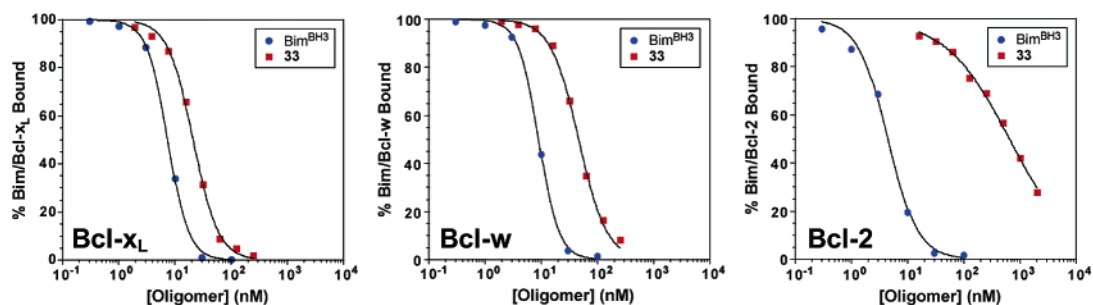


Figure 9. Surface plasmon resonance-based competition binding assays. Competition of $(\alpha/\beta+\alpha)$ -peptide **33** (red) or Bim^{BH3} (blue; sequence in ref 16a) with immobilized Bim^{BH3} for binding to Bcl-x_L, Bcl-w, or Bcl-2. IC₅₀ values reported in text are calculated from nonlinear curve-fitting of the competition binding data (black curves).

IC₅₀ values to small changes in $(\alpha/\beta+\alpha)$ -peptide structure (Tables 1–3). This sensitivity suggests that these oligomers target a well-defined binding site on Bcl-x_L; ligands that bind nonspecifically (e.g., via an aggregated state) generally manifest flat structure–affinity landscapes.¹ Finally, the Hill coefficients for competition FP isotherms of $(\alpha/\beta+\alpha)$ -peptides were ~ 1 in each case (largest Hill coefficient = 1.4 for $(\alpha/\beta+\alpha)$ oligomer **14**; average Hill coefficient for all $(\alpha/\beta+\alpha)$ -peptides = 0.9 ± 0.1), which suggests that these ligands interact with a single site on Bcl-x_L.

Binding Selectivity among Anti-apoptotic Bcl-2 Family Proteins. BH3 peptides from pro-apoptotic Bcl-2 family proteins differ from one another in their binding profiles among anti-apoptotic Bcl-2 family proteins.¹⁶ The Bak BH3 domain, for example, binds very strongly to Mcl-1, less strongly to Bcl-x_L, moderately to Bcl-w, and weakly, if at all, to Bcl-2. In contrast, the Bad BH3 domain binds weakly to Mcl-1, and tightly to Bcl-x_L, Bcl-w, and Bcl-2. The Bim BH3 domain binds very strongly to all four of these anti-apoptotic family members. We used surface plasmon resonance (SPR) to compare the binding of $(\alpha/\beta+\alpha)$ -peptide **33** among anti-apoptotic proteins Bcl-x_L, Bcl-2, Bcl-w, and Mcl-1. Foldamer **33** was selected for this comparison because it displays the highest affinity for Bcl-x_L in the FP assay among all of the $(\alpha/\beta+\alpha)$ -peptides we evaluated.

The SPR assay involves competition between the $(\alpha/\beta+\alpha)$ -peptide, in solution, and a surface-immobilized Bim BH3 α -peptide (Bim^{BH3}) for binding to an anti-apoptotic protein.^{16a} The results are presented in terms of an IC₅₀ for prevention of protein binding to the immobilized α -peptide. As expected on the basis of our FP studies, **33** potently inhibited binding of Bcl-x_L to immobilized Bim^{BH3} (IC₅₀ by SPR = $0.018 \mu\text{M}$; Figure 9). Binding of Bcl-w to Bim^{BH3} was inhibited almost as effectively (IC₅₀ = $0.041 \mu\text{M}$), but **33** appeared to have a considerably lower affinity for Bcl-2 (IC₅₀ = $0.85 \mu\text{M}$). No interaction of **33** with Mcl-1 could be detected (IC₅₀ > $10 \mu\text{M}$, not shown). In contrast to **33**, Bim^{BH3} bound tightly to all four anti-apoptotic Bcl-2 family proteins (IC₅₀ values = 0.004 – $0.014 \mu\text{M}$), consistent with previous studies.^{16a,c}

The pronounced selectivity displayed by **33** among anti-apoptotic Bcl-2 family proteins supports a model in which tight binding to Bcl-x_L and Bcl-w involves a specific interaction with the BH3-recognition cleft on these proteins (if **33** acted by denaturing proteins or binding nonspecifically, this oligomer would presumably be nonselective among Bcl-2 family proteins, especially because these proteins are homologous). The selectivity profile of **33** is similar to that manifested by the BH3 domain of Bik, and also appears to be a hybrid of the profiles for the

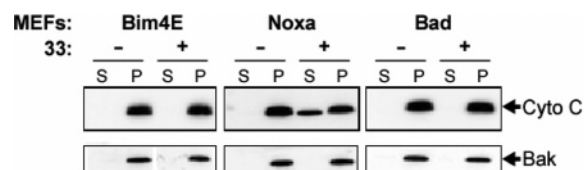


Figure 10. Cytochrome C (Cyto C) release assays. Extracts derived from mouse embryonic fibroblasts (MEFs) that overexpress a biologically inert Bim mutant (Bim4E, ref 16a), Noxa, or Bad were treated with (+) or without (–) $10 \mu\text{M}$ $(\alpha/\beta+\alpha)$ -peptide **33**. Cellular material was fractionated, and cytochrome C was measured in soluble (S) and particulate (P) fractions, indicating cyto C released from and retained by mitochondria, respectively. Bak was present in mitochondrial (P) fractions in all experiments.

Bad and Bak BH3 domains. Like the BH3 domains of Bad and Bak, **33** displays high affinity for Bcl-x_L and Bcl-w. Oligomer **33** shares with the Bak BH3 domain a significantly lower affinity for Bcl-2 relative to Bcl-x_L or Bcl-w, whereas the BH3 domain of Bad binds almost equipotently to Bcl-x_L, Bcl-w, and Bcl-2. On the other hand, **33** shares with Bad BH3 an inability to bind to Mcl-1, whereas Bak BH3 binds to this protein with high affinity.

Selective Disruption of Bcl-x_L/BH3 Interaction in a Biological Environment. The experiments described above show that appropriately designed $(\alpha/\beta+\alpha)$ -peptide ligands can inhibit the binding of BH3 domain-derived α -peptides to anti-apoptotic Bcl-2 family proteins in aqueous buffer. We sought to determine whether optimized $(\alpha/\beta+\alpha)$ -peptide antagonist **33** could block the interaction of Bcl-x_L with pro-apoptotic proteins in a biological milieu and thereby elicit a pro-apoptotic effect. Toward this end, we measured the ability of **33** to cause cytochrome C release from mitochondria in crude lysates of mouse embryonic fibroblasts (MEFs), a process that constitutes a model of apoptosis induction and that is regulated by Bcl-2 family protein–protein interactions.^{16a} These experiments were performed with cell lysates because we did not expect $(\alpha/\beta+\alpha)$ -peptide **33** to move unassisted across an intact cell membrane.

Mouse embryonic fibroblasts are normally protected from Bak-induced apoptosis by Mcl-1 and Bcl-x_L, both of which bind tightly to Bak.^{16b} Because our SPR results show that $(\alpha/\beta+\alpha)$ -peptide **33** binds strongly to Bcl-x_L but not to Mcl-1, we did not expect **33**, alone, to induce cytochrome C release from mitochondria in normal MEF lysates. We therefore used mouse fibroblasts that overexpress the pro-apoptotic protein Noxa, which binds tightly to the BH3-recognition cleft of Mcl-1 but not to Bcl-x_L.^{16a,c} In the presence of Noxa, $(\alpha/\beta+\alpha)$ -peptide **33** was able to induce cytochrome C release from mitochondria (Figure 10). No release was observed, however, when **33** was added to lysates derived from cells that overexpress Bad (which

selectively binds to Bcl-x_L but not to Mcl-1) or a biologically inert mutant of Bim (which does not bind to any pro-survival Bcl-2 family proteins).^{16a} These results suggest that ($\alpha/\beta+\alpha$)-peptide **33** can disrupt interactions of Bcl-x_L with pro-apoptotic Bcl-2 family proteins in cytosolic extracts, allowing Bak to induce mitochondrial membrane permeability. The observation that **33** induces cytochrome C release only in the presence of Noxa shows that the biological effect of **33** is due to specific targeting of Bcl-x_L.

Discussion

The results presented above reveal several important principles behind the design of foldamer-based ligands for a specific protein surface, the BH3-recognition cleft of Bcl-x_L. This target site on Bcl-x_L evolved to recognize α -helical segments on partner proteins, forming contacts distributed over three successive α -helical turns on the natural ligands.^{12,14} We have tried to mimic this elongated recognition surface with helical foldamers. Of four foldamer scaffolds evaluated for binding to Bcl-x_L, the β -peptide 12- and 14-helices and the α/β -peptide 11- and 14/15-helices, only the 14/15-helix appears to be suitable for this purpose;^{18e} we have identified 14/15-helical α/β -peptides with micromolar affinity for the BH3-recognition cleft of Bcl-x_L ($K_i = 4 \mu\text{M}$ for **4**). Our tightest-binding Bcl-x_L ligands ($K_i = 0.0022 \mu\text{M}$ for **33**) are chimeric, containing an α/β -peptide segment fused to an α -peptide segment. These results indicate that the BH3 domain is not well mimicked in its entirety by the α/β - or β -peptide scaffolds we have investigated. In contrast, the β -peptide 14-helix and 12-helix have proven to be competent to interfere with other protein–protein recognition processes that involve α -helices (albeit with lower potency than is displayed by the best ($\alpha/\beta+\alpha$)-peptides described here).^{18a–d}

The success of our chimeric approach to Bcl-x_L ligand design suggests that mimicry of large protein-binding epitopes, such as a BH3 domain, may be best accomplished via replacement of short segments of the epitope with distinct foldameric scaffolds. The α -peptide backbone is flexible, and a “regular” secondary structure such as an α -helix can contain significant local distortion from idealized backbone torsion angles, as is seen for Bak^{BH3} in complex with Bcl-x_L.^{14a} Foldamer backbones often contain conformationally constrained subunits,^{7,8,15} such as cyclic β -amino acid residues,⁸ which do not allow the range of local backbone conformations accessible to an α -peptide segment. Therefore, different portions of a large protein epitope may require different foldamer scaffolds for effective mimicry. This view suggests that our ability to generate foldameric antagonists of protein–protein interactions will be enhanced by the identification of a variety of foldamer scaffolds that offer distinct ways to arrange side chains (and perhaps backbone elements).

We have used “alanine scanning”, a well-established experimental tool for the study of conventional peptides and proteins,²⁹ to develop a structural model for the complex formed between Bcl-x_L and chimeric ($\alpha/\beta+\alpha$)-peptide ligands. Thus, starting from a ligand with high affinity for Bcl-x_L, ($\alpha/\beta+\alpha$)-peptide **6**, we systematically changed each α - and β -residue side chain to a methyl group. The ($\alpha/\beta+\alpha$)-peptide variants were compared via an FP assay, which measures the ability of each compound to displace a fluorophore-labeled α -peptide, derived from the BH3 domain of Bak, from the BH3-recognition cleft of Bcl-

x_L. The results implicate four side chains on **6**, those of Arg-4, Leu-6, Asp-11, and Phe-13, as forming particularly important contacts with Bcl-x_L.

A variation on alanine scanning, which we designate “hydrophile scanning”, was developed to identify additional hydrophobic residues of ($\alpha/\beta+\alpha$)-peptides that interact with the binding cleft on Bcl-x_L. In the hydrophile scan, lipophilic side chains are systematically replaced with hydrophilic analogues; burial of a hydrophilic residue in a largely lipophilic environment is expected to be unfavorable. Thus, hydrophile scanning can provide structural insights complementary to those gained from alanine scanning, as illustrated by our findings with ACPC replacements in ($\alpha/\beta+\alpha$)-peptide ligands for Bcl-x_L. Although the effects of ACPC \rightarrow β^3 -hAla replacements (alanine scanning) indicated that the side chains of these residues are of low importance for binding to Bcl-x_L, effects of ACPC \rightarrow APC replacements (hydrophile scanning) suggested that ACPC residues at positions 3 and 7 are nevertheless buried in the ($\alpha/\beta+\alpha$)-peptide/Bcl-x_L interface. This apparent discrepancy raises the possibility that burial of ACPC-3 and ACPC-7 in the hydrophobic binding cleft of Bcl-x_L, which is likely to be favorable, is offset by unfavorable changes in the protein/ligand interface. For example, the ACPC rings may be too large to permit optimal complementarity with the BH3-recognition cleft along the entire length of an ($\alpha/\beta+\alpha$)-peptide ligand. In other words, globally optimal positioning of an ($\alpha/\beta+\alpha$)-peptide in the Bcl-x_L cleft may require locally nonoptimal interactions between protein and ligand and/or within each partner. This hypothesis is supported by our observation that alanine mutations of residues other than ACPC in ($\alpha/\beta+\alpha$)-peptide **6** are not as deleterious to binding as are Ala replacements of analogous residues in the Bak BH3 domain.^{14a} The above model might explain why mutation of ACPC residues to β^3 -hAla resulted in only small decreases in Bcl-x_L affinity: replacing the cyclopentyl ring with a methyl group may allow improved overall protein/ligand complementarity, resulting from increased backbone flexibility and/or less steric bulk at position 3 or 7, to compensate partially for the diminution of hydrophobic interaction surface at these positions.

Hydrophile scanning may prove to be a generally useful complement to alanine scanning for probing peptide/protein, protein/protein, and foldamer/protein interfaces. The impact of changing a large nonpolar side chain to a methyl group indicates whether the original side chain contributes favorably to the binding energy.²⁹ Substantial decreases in affinity arising from such Ala mutations therefore imply burial of the large nonpolar side chain at the original interface, but the converse is not necessarily true. It is commonly observed among protein–protein and peptide–protein interfaces (including the Bad^{BH3}/Bcl-x_L interface) that some hydrophobic side chains known to be buried in the complex can nevertheless be replaced by a methyl group without significant loss in affinity.^{14b,29,37} In contrast to alanine scanning, mutation of a hydrophobic residue to a hydrophilic residue should indicate whether the original side chain is buried in a nonpolar environment in the bound state regardless of the side chain’s net energetic contribution to binding, so long as the hydrophobic \rightarrow hydrophilic substitution does not affect the overall conformational stability of the ligand (a comparable assumption must be made for alanine scanning²⁹).

(37) Greenspan, N. S.; Di Cera, E. *Nat. Biotechnol.* **1999**, *17*, 936–937.

Varadarajan and co-workers have recently implemented a technique similar to hydrophile scanning for examination of hydrophobic side chain burial within a folded protein.³⁸ This group found that hydrophobic \rightarrow hydrophilic substitutions are better indicators of side chain burial than are Ala mutations. Alanine scanning mutagenesis data have been used to provide constraints in protein–protein docking calculations;³⁹ we believe that hydrophile scanning data could provide valuable additional constraints in such calculations.

Results of our alanine and hydrophile scanning analyses led us to $(\alpha/\beta+\alpha)$ -peptide **24**, which displays significantly improved affinity for Bcl-x_L relative to **6**, as judged by results from the competition FP assay. We used a computational docking method to generate a structural model for binding of **24**, in a helical conformation, to the BH3-recognition cleft of Bcl-x_L. All of our mutational results can be rationalized qualitatively on the basis of this model. The structural hypothesis that $(\alpha/\beta+\alpha)$ -peptide **24** binds to Bcl-x_L in a mode that mimics the binding of natural BH3 domains gives rise to several predictions, which we tested by means of a variety of experimental approaches.

The Bcl-x_L/**24** complexation model is based on the assumption of a 1:1 protein:ligand binding stoichiometry. Analytical ultracentrifugation shows that the binding stoichiometry is indeed 1:1, so long as the medium contains a non-ionic detergent. Non-ionic detergents are commonly included in buffers to be used for protein manipulation and assay to block undesired and nonspecific protein aggregation. Recently, it has been demonstrated that detergent can prevent aggregation of small molecules that are intended to bind in specific ways to proteins; such aggregation can give rise to artifactual results in protein inhibition assays.³⁶ Self-association of proteins or of small molecules in aqueous solution is generally driven by burial of hydrophobic surfaces, and the inhibition of self-association by detergent presumably arises because the detergent acts as a kind of hydrophobic buffer. In addition to ligand or protein self-association, detergent can presumably block nonspecific protein–ligand interactions driven by hydrophobic interactions. Indeed, AU analysis in the absence of detergent indicates a Bcl-x_L:**24** binding stoichiometry of nearly 1:2, and we believe that the additional ligand association revealed under these conditions arises from nonspecific interaction. The interior of a cell offers multiple sources of hydrophobic buffering, such as lipid bilayers and promiscuous hydrophobe-binding proteins; the use of detergents for in vitro studies presumably mimics this aspect of in vivo conditions.

Our binding data from the competition FP assay point to the BH3-recognition cleft on the surface of Bcl-x_L as the binding site for $(\alpha/\beta+\alpha)$ -peptides. The FP studies show that nanomolar concentrations of $(\alpha/\beta+\alpha)$ -peptide ligands can prevent binding of a fluorophore-labeled Bak^{BH3} probe to Bcl-x_L and that this inhibition displays dose–response relationships consistent with single-site binding (Hill coefficients \sim 1). An independent competition assay format based on SPR (i.e., not reliant on fluorescence measurement or fluorophore tags) indicated a comparable ability of our most potent $(\alpha/\beta+\alpha)$ -peptide, **33**, to antagonize the Bim^{BH3}/Bcl-x_L interaction.

The Bcl-x_L/**24** binding model features high complementarity between the surface presented by the helical $(\alpha/\beta+\alpha)$ -peptide ligand and the surface presented by the BH3-recognition cleft on the protein. This model would be supported by the observation that $(\alpha/\beta+\alpha)$ -peptides related to **24** are selective in binding to Bcl-x_L relative to other anti-apoptotic Bcl-2 family proteins. (Lack of specificity among these proteins, however, would not necessarily invalidate our model, because some natural BH3 domains, such as that from Bim, bind tightly to a variety of anti-apoptotic Bcl-2 family proteins (Figure 9).¹⁶) The competition SPR assays did, in fact, reveal that $(\alpha/\beta+\alpha)$ -peptide **33** is selective for binding to Bcl-x_L and Bcl-w. The affinity of **33** for Bcl-2 is substantially lower, and there is no detectable affinity for Mcl-1. The selectivity of **33** among anti-apoptotic Bcl-2 family proteins is similar to that of natural BH3 domains, (e.g., Bik), which highlights the prospect of using this and other foldamers with BH3 like selectivity profiles or novel selectivities as biological research tools.

Binding of $(\alpha/\beta+\alpha)$ -peptides to the BH3-recognition cleft of Bcl-x_L, demonstrated in experiments carried out with purified protein, predicts that these oligomers should be able to block interactions between Bcl-x_L and pro-apoptotic proteins in a biological environment and perhaps elicit an apoptotic response. These predictions were tested by exposing mouse embryonic fibroblast lysates to $(\alpha/\beta+\alpha)$ oligomer **33**. In lysates derived from fibroblasts engineered so that the primary anti-apoptotic effect is exerted by Bcl-x_L, exposure to $(\alpha/\beta+\alpha)$ -peptide **33** stimulated the release of cytochrome C from mitochondria, presumably by displacing a pro-apoptotic Bcl-2 family protein (e.g., Bak) from the BH3-recognition cleft of Bcl-x_L. Control experiments showed that **33** does not induce cytochrome C release when both Mcl-1 and Bcl-x_L are available to sequester Bak, possibly because **33** cannot displace Bak from Mcl-1. These control experiments strongly support the interpretation that the impact of **33** on mitochondria depends on a specific interaction between this $(\alpha/\beta+\alpha)$ -peptide and Bcl-x_L.

Conclusions and Future Prospects

The results presented here, along with other recent reports,^{15,18} support the emerging view that foldamers represent a versatile set of scaffolds from which inhibitors of protein–protein interactions can be developed. Further exploration of this hypothesis will require extension of foldamer-based approaches to new targets, and the identification of new foldamer families that provide distinct ways to arrange binding elements in space. α -Helices that play central roles in protein–protein interactions represent not one but rather a family of structures to be mimicked by unnatural scaffolds. Conformational variation among these α -helices, illustrated by the difference between the helical epitope presented by p53 to hDM2¹⁹ and the helical epitope presented by Bak to Bcl-x_L,¹⁴ most probably arises from the intrinsic flexibility of the α -peptide backbone, which can distort locally to optimize complementarity to a partner protein surface. The diversity among natural α -helices involved in protein–protein recognition suggests the need for a corresponding diversity in strategies for creating pre-organized foldamer helices that can be used to develop ligands with high affinity and high specificity for target proteins.

Bcl-x_L and related anti-apoptotic proteins represent an attractive set of targets for continued research aimed at identifying

(38) Bajaj, K.; Chakrabarti, P.; Varadarajan, R. *Proc. Natl. Acad. Sci. U.S.A.* **2005**, *102*, 16221–16226.

(39) Dominguez, C.; Boelens, R.; Bonvin, A. M. J. *J. Am. Chem. Soc.* **2003**, *125*, 1731–1737.

foldamers that can mimic α -helical epitopes. Our finding that the α/β -peptide 14/15-helix is effective for occupying only $\sim 60\%$ of the BH3-recognition cleft on Bcl-x_L identifies one challenge to be met in future work: discovery of new foldamer scaffolds that can replace the C-terminal α -peptide segment in chimeric ($\alpha/\beta+\alpha$) ligands while retaining high Bcl-x_L affinity and high proteolytic stability.⁴⁰ The achievements reported here substantially decrease the susceptible portion of the ligand, from 16 α -residues (in Bak^{BH3}) to 6 (in ($\alpha/\beta+\alpha$)-peptide **33**), which represents substantial progress toward the ultimate goal of metabolic stability.

Another challenge is highlighted by the selectivity displayed by **33** for Bcl-x_L and Bcl-w relative to Bcl-2 and Mcl-1. Foldameric ligands selective for the BH3-recognition clefts of one or both of the latter two targets would be valuable, and the process of identifying those ligands should enhance our understanding of the factors responsible for both affinity and selectivity in binding to specific protein surfaces. The attraction of the Bcl-2 family for these fundamental studies is enhanced by the considerable structural data available for proteins in this family and their complexes.¹² Furthermore, new high-resolution structures are likely to emerge because of the broad attention received by these proteins from the scientific community. Because many aspects of the functional significance of Bcl-2 family protein interactions remain unclear in terms of cellular fate, new protein-specific ligands could prove useful as tools for basic biological research.

This work demonstrates that foldamer-based ligands for a specific protein-recognition site can be discovered and optimized via “test tube” experiments and that such ligands can subsequently be shown to function in a biological context. The science of developing synthetic ligands that interfere with the binding of one protein to another is currently in a primitive state.¹ Efforts of the type described here, focusing mostly on basic studies with purified proteins, will be essential for continued progress in this area. The molecular-level understanding generated by such basic research provides the concepts and tools that will be necessary, in the long term, to create agents that disrupt disease-related protein–protein interactions in a clinically useful way.

Experimental Section

General. Fmoc-L- α -amino acids and NovaSyn TGR resin were purchased from NovaBiochem (San Diego, CA). Fmoc- β -amino acids were synthesized using previously described routes.⁴¹ Piperidine was purchased from Acros (Morris Plains, NJ) or Aldrich (Milwaukee, WI). 5-Carboxyfluorescein and BODIPY-TMR-X were purchased from Molecular Probes (Eugene, OR). HPLC-grade acetonitrile was purchased from Burdick and Jackson (Muskegon, MI). *N,N*-Dimethylformamide (DMF), dichloromethane (DCM), HBTU, HOBt, trifluoroacetic acid (TFA), and all other chemicals and reagents were purchased from Aldrich.

- (40) (a) Frackenhohl, J.; Arvidsson, P. I.; Schreiber, J. V.; Seebach, D. *ChemBioChem* **2001**, *2*, 445–455. (b) Hook, D. F.; Bindschadler, P.; Mahajan, Y. R.; Sebesta, R.; Kast, P.; Seebach, D. *Chem. Biodiversity* **2005**, *2*, 591–632.
- (41) β^3 -Amino acid synthesis: (a) Seebach, D.; Overhand, M.; Kuehnle, F. N. M.; Martinoni, B.; Oberer, L.; Hommel, U.; Widmer, H. *Helv. Chim. Acta* **1996**, *79*, 913–941. (b) Mueller, A.; Vogt, C.; Sewald, N. *Synthesis* **1998**, *6*, 837–841. β^2 -Amino acid synthesis: (c) Lee, H.-S.; Park, J.-S.; Kim, B. M.; Gellman, S. H. *J. Org. Chem.* **2003**, *68*, 1575–1578. Cyclic β -amino acid synthesis: (d) LePlae, P. R.; Umezawa, N.; Lee, H.-S.; Gellman, S. H. *J. Org. Chem.* **2001**, *66*, 5629. (e) Lee, H.-S.; LePlae, P. R.; Porter, E. A.; Gellman, S. H. *J. Org. Chem.* **2001**, *66*, 3597–3599. (f) Schinnerl, M.; Murray, J. K.; Langenhan, J. M.; Gellman, S. H. *Eur. J. Org. Chem.* **2003**, *4*, 721–726.

Peptide Synthesis. Peptides were synthesized in 1.5-mL solid-phase extraction tubes from Alltech (Deerfield, IL) on NovaSyn TGR resin, to afford upon cleavage from the resin C-terminal primary amides. A vacuum manifold was used to wash the resin with DMF and DCM between coupling and deprotection steps, allowing up to 48 peptides to be synthesized in parallel. The synthesis of ($\alpha/\beta+\alpha$)-peptide **24** (Ac-APC-Ala-ACPC-Arg-ACPC-Leu-ACPC-Lys- β^3 hNle-Gly-Asp-Ala-Phe-Asn-Arg-NH₂) on a 5 μ mol scale is representative: ~ 20 mg of NovaSyn TGR resin (reported loading = 0.25 mmol/g) was swelled for 1 h in DCM. After the resin was washed with DCM and DMF, 3 equiv (15 μ mol) of Fmoc-L- α -Arg-OH (Pbf-protected) and 3 equiv (15 μ mol) of HBTU dissolved in 250 μ L of DMF were added to the resin. DIEA (60 μ L; 0.5 M solution in DMF) and HOBt (30 μ L; 0.5 M solution in DMF) were sequentially added to initiate the coupling, which was allowed to proceed for > 1 h at room temperature on a LabQuake rocker. After the resin was washed with DCM and DMF, Fmoc deprotection was accomplished by adding to the resin ~ 0.5 mL of 20% (v/v) piperidine in DMF and rocking for 15–20 min. Subsequent couplings and deprotections proceeded in a manner similar to the first coupling and deprotection. N-Terminal acetylation of peptides proceeded for ~ 3 h by addition of 0.5 mL of 5:1:14 (v/v/v) Ac₂O:Et₃N:DCM to the resin bearing the final N-deprotected peptide. **Flu-Ahx-24** was synthesized by coupling Fmoc- ϵ -amino hexanoic acid followed by 5-carboxyfluorescein to N-deprotected **24** using the coupling/deprotection conditions described above. All peptides were cleaved from the resin for ~ 3 h using a trifluoroacetic acid (TFA) cocktail containing 2.5% triisopropylsilane and 2.5% water. After evaporation of TFA under a steady nitrogen stream, the crude products were dissolved in DMSO and purified by semipreparative, reverse-phase HPLC performed with a C4 column (Vydac, Anaheim, CA) and eluting with gradients of acetonitrile/0.1% TFA (B solvent) in water/0.1% TFA (A solvent). Fractions were lyophilized to yield the final peptide products as dry powders. Purity was estimated at $> 90\%$ by analytical HPLC analysis, and peptide identity was confirmed by MALDI-TOF mass spectrometry (see Supporting Information).

Fluorescence Polarization Assays. Fluorescence polarization experiments were performed using a Perkin-Elmer EnVision multi-label plate reader (Wellesley, MA) with polarized filters and optical modules for BODIPY-TMR ($\lambda_{\text{excitation}}$, 531 nm; $\lambda_{\text{emission}}$, 595 nm). The G-factor for all FP experiments was set to 1. The Bcl-x_L construct used in FP assays, which lacked the C-terminal transmembrane domain and a non-essential loop, was expressed in *E. coli* as previously described.⁴² The BODIPY^{TMR}-labeled Bak^{BH3} peptide used as the probe in competition FP experiments was synthesized in solution by reacting the unlabeled Bak^{BH3} peptide (H₂N-GQVGRQLAIIGDDINR-CONH₂) with excess BODIPY-TMR-X, an amine-reactive, succinimidyl ester form of the BODIPY-TMR fluorophore, in DMF with 2.5% Et₃N. BODIPY^{TMR}-Bak^{BH3} was purified by reverse-phase HPLC. The binding dissociation constant (K_d) of BODIPY^{TMR}-Bak^{BH3} for Bcl-x_L, determined by a direct-binding FP assay, was 4 ± 1.8 nM. Competition FP assays were conducted in 96-well plates with final assay concentrations of Bcl-x_L and BODIPY^{TMR}-Bak^{BH3} probe fixed at 20 and 33 nM, respectively, in assay buffer (20 mM phosphate, 1 mM EDTA, 50 mM NaCl, 0.2 mM NaN₃, 0.5 mg/mL Pluronic F-68, pH 7.4).²¹ Final assay concentrations of inhibitors, added as a 5–10 mM stock solution in DMSO (quantified by peptide weight), ranged from 400 to 0.0002 μ M; the final assay concentration of DMSO was 4% (v/v). Assay plates were incubated in the dark for ~ 3 h at room temperature before being analyzed by the plate reader. Raw competition FP data were converted to percent inhibition of the BODIPY^{TMR}-Bak^{BH3}/Bcl-x_L interaction, and binding data were fit in GraphPad Prism 4.0 (San Diego, CA) by using the one-site competition binding model to determine IC₅₀ values and

- (42) Enyedy, I. J.; Ling, Y.; Nacro, K.; Tomita, Y.; Wu, X.; Cao, Y.; Guo, R.; Li, B.; Zhu, X.; Huang, Y.; Long, Y.-Q.; Roller, P. P.; Yang, D.; Wang, S. *J. Med. Chem.* **2001**, *44*, 4313–4324.

associated 95% confidence intervals. Inhibitor dissociation constant (K_i) values were calculated from IC_{50} values according to ref 24.

Docking Studies. Docking studies were performed with the Flexdock module in the Sybyl molecular modeling program (Tripos Inc., St. Louis, MO). A three-dimensional model of oligomer **24** was first constructed by fusing a model of a 14/15-helical α/β -peptide^{8a} to the C-terminal residues of Bak^{BH3}, extracted from the Bak^{BH3}/Bcl-x_L complex (PDB accession code: 1BXL).^{14a} The model of **24** was then modified to display the appropriate side chains, energy-minimized in vacuo to the nearest local minimum, and manually placed into the BH3-recognition cleft of Bcl-x_L. This manually docked complex served as the input for 10 Flexdock runs (25 000 generations each, all other parameters set to their default values). All side chain torsional angles in the ligand were allowed to rotate, while the backbone was fixed. The conformation of Bcl-x_L (the receptor) was also fixed. Each run generated 20 low-energy docked structures; the structure of overall lowest energy is shown in Figure 6.

Analytical Ultracentrifugation. Analytical ultracentrifugation (AU) studies were conducted with a Beckman XLA ultracentrifuge at 25 °C. We investigated binding of **Flu-Ahx-24** to Bcl-x_L in two buffer systems by AU: (1) PBS with 2 mM β -mercaptoethanol and (2) a 1:8 dilution of this buffer into that used for FP assays. For each buffer system, we generated three samples for AU analysis with the following ligand:protein ratios: 6 μ M:4 μ M, 12 μ M:4 μ M, and 6 μ M:0 μ M. All samples contained 4% (v/v) DMSO from addition of **Flu-Ahx-24**. These samples and a buffer/DMSO blank were loaded into four 1.2 cm cells and centrifuged at rotor speeds of 30 000–40 000 rpm in the AU instrument; sedimentation of the bound fraction of **Flu-Ahx-24** to the bottom of the cells was monitored by measuring absorbance of Flu at 477 nm. After 10–12 h, the bound **Flu-Ahx-24**/Bcl-x_L complex was completely sedimented away from the meniscus of the AU cell, as indicated by linear regression analysis, leaving free **Flu-Ahx-24** at the meniscus. Binding stoichiometry was calculated by comparing the amount of free ligand at the meniscus for the three protein/ligand samples described above. To estimate the aggregation state of **Flu-Ahx-24** alone (6 μ M), a nonlinear curve was fit to AU data acquired with rotor speeds of 30 000 and 40 000 rpm using the following equation:

$$c_r = c_o \exp[M(1 - \nu\rho)\omega^2(r^2 - r_o^2)/(2RT)]$$

Parameter c_r is the concentration (in absorbance units) at radial position r , c_o is the concentration at an arbitrary reference position r_o near the meniscus (measured at a low rotor speed, 3000 rpm), ν is the partial specific volume (0.740 mL/g, calculated on the basis of peptide composition), ρ is the solvent density (0.9983 g/mL, estimated on the basis of buffer composition), ω is the rotor speed, R is the gas constant, and T is the temperature. Molecular weight estimates were obtained from the fitted parameter, M . The estimated molecular weight of **Flu-Ahx-24**, based on linear regression, was 70–100% that of the expected molecular weight of a monomer in both buffer systems, implying that this oligomer does not aggregate under these conditions.

Competition SPR Binding Assays. The Bcl-2 family proteins used for SPR assays included biologically active C- and/or N-terminal truncation mutants of Bcl-x_L, Mcl-1, Bcl-2, and Bcl-w, expressed in *E. coli* as previously described.^{16a} Competition assays using the Biacore

optical biosensor were performed essentially as described.^{16a} Briefly, pro-survival proteins (0.010 μ M) were incubated with varying concentrations of inhibitory oligomer (**33** or Bim^{BH3}) for 2 h in binding buffer (10 mM Hepes, 150 mM NaCl, 3.4 mM EDTA, 0.005% Tween 20, pH 7.4) prior to injection onto a CM-5 sensor chip on which either a wild-type Bim BH3 peptide or an inert Bim BH3 mutant peptide had been immobilized. Specific binding of the Bcl-2 family protein to the surface in the presence and absence of inhibitors was quantified by subtracting the signal arising from the Bim mutant channel from that arising from the wild-type Bim channel. The ability of **33** or Bim^{BH3} to prevent protein binding to immobilized Bim BH3 was expressed as the IC_{50} , as calculated by nonlinear curve-fitting of the data with Kaleidagraph.

Cytochrome C Release Assays. Mouse embryonic fibroblasts stably expressing human Noxa, mouse Bad, or an inert, human Bim mutant were established by retroviral infection with constructs in which the expression of these pro-apoptotic proteins was linked to a hygromycin selection cassette in a modified pMIG vector.^{16a} Cells ($\sim 10^7$) were pelleted and lysed in 0.05% (w/v) digitonin-containing lysis buffer (20 mM Hepes, 100 mM KCl, 5 mM MgCl₂, 1 mM EDTA, 1 mM EGTA, 250 mM sucrose, pH 7.2), supplemented with protease inhibitors (Roche, Indianapolis, IN), for 10 min on ice. The mitochondria-containing crude lysates were left untreated or incubated with **33** (10 μ M) at 30 °C for 1 h before pelleting. The supernatant was saved as the soluble (S) fraction, while the pellet (P), which contained intact mitochondria, was solubilized in RIPA buffer. Both the soluble and the pellet fractions were subjected to SDS-PAGE, and proteins were transferred to nitrocellulose membranes, which were immunoblotted using a mouse monoclonal anti-cytochrome C antibody (7H8.2C12; BD Biosciences, San Jose, CA) followed by rabbit polyclonal anti-Bak antibody (B5929; Sigma, Milwaukee, WI). The membranes were then probed with horseradish peroxidase-conjugated anti-mouse Ig or anti-rabbit Ig antibodies, and associated proteins were detected by chemiluminescence.

Acknowledgment. This research was funded by the NIH (GM56414; to S.H.G.), the Australian NHMRC (Program Grant 257502; and fellowships to D.C.S.H. and W.D.F.), NCI (CA80188, CA43540; to J. M. Adams and S. Cory), and the Leukemia and Lymphoma Society (SCOR 7015-02; to D.C.S.H.). We are grateful to Y. Udea (Georgetown) for assistance with protein expression. The plate reader used for FP assays is in the UW-Madison W.M. Keck Center for Chemical Genomics. The analytical ultracentrifuge is part of the Biophysics Instrumentation Facility at UW-Madison. N.U. was supported in part by a Research Fellowship for Young Scientists from the Japan Society for the Promotion of Science. An NSF predoctoral fellowship partially supported J.D.S.

Supporting Information Available: Experimental details, peptide synthesis protocols and characterization data, FP binding data, and complete ref 3c. This material is available free of charge via the Internet at <http://pubs.acs.org>.

JA0662523